

1 **Short Title:** Genetic Control of Transcript Levels in Tomato

2

3 **Corresponding author:**

4 Neelima R. Sinha

5 Department of Plant Biology

6 1002 Life Sciences

7 One Shields Ave.

8 Phone: (530) 754-8441

9 Fax: (530) 752-5410

10 e-mail: nrsinha@ucdavis.edu

11

12 **Research area:** Genes, Development and Evolution

13

14

15

16

17

18

19

20

21

22

23

24

25 **Title: eQTL regulating Transcript Levels Associated with Diverse**
26 **Biological Processes in Tomato**

27

28 Aashish Ranjan^{#a¶}, Jessica M. Budke^{¶b}, Steven D. Rowland[¶], Daniel H.
29 Chitwood^{#c}, Ravi Kumar^{#d}, Leonela Carriedo, Yasunori Ichihashi^{#e}, Kristina
30 Zumstein, Julin N. Maloof, and Neelima R. Sinha

31 Department of Plant Biology, University of California at Davis, Davis, California,
32 United States of America

33

34 [¶]These authors contributed equally to this work.

35

36 **Summary:** The combined use of genetic mapping and transcript coexpression
37 analysis was used to identify genetic hotspots that regulate transcript levels of
38 genes linked to diverse biological processes.

39

40

41

42

43

44 **Footnotes:**

45 **Funding information:** This work is supported through a National Science
46 Foundation grant (IOS-0820854) awarded to NRS and JNM. DHC was a fellow of
47 the Life Sciences Research Foundation funded through the Gordon and Betty
48 Moore Foundation. JMB is a recipient of Katherine Esau Postdoctoral Fellowship
49 at UC Davis.

50 **Present Address:**

51 #^a : National Institute of Plant Genome Research, New Delhi, India.

52 #^b : Department of Ecology and Evolutionary Biology, University of Tennessee,
53 Knoxville, Tennessee, United States of America.

54 #^c : Donald Danforth Plant Science Center, St. Louis, Missouri, United States of
55 America.

56 #^d : Novozymes, Davis, California, United States of America.

57 #^e : RIKEN Center for Sustainable Resource Science, Yokohama, Kanagawa,
58 Japan.

59

60 **Corresponding author email:** nrsinha@ucdavis.edu

61

62

63

64 **Abstract**

65 Variation in gene expression, in addition to sequence polymorphisms, is known to
66 influence developmental, physiological and metabolic traits in plants. Genetic
67 mapping populations have facilitated identification of expression Quantitative
68 Trait Loci (eQTL), the genetic determinants of variation in gene expression
69 patterns. We used an introgression population developed from the wild desert-
70 adapted *Solanum pennellii* and domesticated tomato *Solanum lycopersicum* to
71 identify the genetic basis of transcript level variation. We established the effect of
72 each introgression on the transcriptome, and identified ~7,200 eQTL regulating
73 the steady state transcript levels of 5,300 genes. Barnes-Hut *t*-distributed
74 stochastic neighbor embedding clustering identified 42 modules revealing novel
75 associations between transcript level patterns and biological processes. The
76 results showed a complex genetic architecture of global transcript abundance
77 pattern in tomato. Several genetic hotspots regulating a large number of
78 transcript level patterns relating to diverse biological processes such as plant
79 defense and photosynthesis were identified. Important eQTL regulating transcript
80 level patterns were related to leaf number and complexity, and hypocotyl length.
81 Genes associated with leaf development showed an inverse correlation with
82 photosynthetic gene expression but eQTL regulating genes associated with leaf
83 development and photosynthesis were dispersed across the genome. This
84 comprehensive expression QTL analysis details the influence of these loci on

85 plant phenotypes, and will be a valuable community resource for investigations

86 on the genetic effects of eQTL on phenotypic traits in tomato.

87

88

89

90

91

92

93

94

95

96

97

98

99

100

101

102

103

104

105 **Introduction**

106 The genetic basis of many qualitative and quantitative phenotypic
107 differences in plants has been associated with sequence polymorphisms and the
108 corresponding changes in gene function. However, differences in the levels of
109 steady state transcripts, without underlying changes in coding sequences, also
110 significantly influence plant phenotypes. Closely related plant species often have
111 little coding sequence divergence, nonetheless the related species often develop
112 unique physiological, metabolic, and developmental characteristics indicating that
113 patterns of gene expression are important in species-level phenotypic variation
114 (Kliebenstein, 2009; Koenig et al., 2013). Phenotypic differences attributed to
115 variations in gene expression patterns have been found to influence disease
116 resistance, insect resistance, phosphate sensing, flowering time, circadian
117 rhythm, and plant development (Kroymann et al., 2003; Werner et al., 2005;
118 Clark et al., 2006; Zhang et al., 2006; Svistoonoff et al., 2007; Chen et al., 2010;
119 Hammond et al., 2011).

120 Global transcript level changes across precise genetic backgrounds have
121 been used to define expression Quantitative Trait Loci (eQTL) by identifying
122 genomic regions responsible for the variation in transcript levels (Jansen and
123 Nap, 2001; Kliebenstein, 2009; Druka et al., 2010; Chitwood and Sinha, 2013).
124 An eQTL is a chromosomal region that drives variation in gene expression
125 patterns (i.e., steady state transcript abundance) between individuals of a genetic
126 mapping population and can be treated as a heritable quantitative trait (Brem et

127 al., 2002; Kliebenstein, 2009; Cubillos et al., 2012). Depending upon the
128 proximity to the gene being regulated, eQTL can be classified into two groups:
129 *cis*-eQTL when the physical location of an eQTL coincides with the location of the
130 regulated gene, and *trans*-eQTL when an eQTL is located at a different position
131 from the gene being regulated (Kliebenstein, 2009). eQTL studies with the model
132 plant *Arabidopsis* showed that *cis*-eQTL have a significant effect on local
133 expression levels, whereas *trans*-eQTL often have global influences on gene
134 regulation (DeCook et al., 2006; West et al., 2007; Holloway and Li, 2010).
135 Global eQTL studies also identified *trans*-acting eQTL hotspots, which contain
136 master regulators controlling the expression of a suite of genes that act in the
137 same biological process or pathway. For example, eQTL hotspots in *Arabidopsis*
138 co-locate with the *ERECTA* locus, which has been shown to pleiotropically
139 influence many traits including those regulating morphology (Keurentjes et al.,
140 2007). Similarly the rice *sub1* locus, which regulates submergence tolerance by
141 controlling internode and leaf elongation, controls the activity of ethylene
142 response factors with significant *trans* effects (Fukao et al., 2006). In addition, the
143 eQTL identified using pathogen challenged tissues in barley were enriched for
144 genes related to pathogen response (Chen et al., 2010; Druka et al., 2010). Thus
145 eQTL analyses have the potential to reveal a genome-wide view of the complex
146 genetic architecture of gene expression regulation, the underlying gene
147 regulatory networks, and may also identify master transcriptional regulators.

148 Cultivated tomatoes, along with their wild-relatives, harbor broad genetic
149 diversity and large phenotypic variability (Moyle, 2008; Ranjan et al., 2012).
150 Wide interspecific crosses bring together divergent genomes and hybridization of
151 such diverse genotypes leads to extensive gene expression alterations compared
152 to either parent. Introgression lines (ILs), developed by crosses between wild-
153 relatives and the cultivated tomato to bring discrete wild-relative genomic
154 segments into the cultivated background, have proved to be a useful genetic
155 resource for genomics and molecular breeding studies. These ILs may vary in
156 the size of introgressed region that may range from a few genes to more than a
157 thousand genes. ILs developed from the wild desert-adapted species *Solanum*
158 *pennellii* and domesticated *Solanum lycopersicum* cv. M82 have proved to be a
159 useful genetic resource (Eshed and Zamir, 1995; Liu and Zamir, 1999). This
160 population has been successfully used to map numerous QTL for metabolites,
161 enzymatic activity, yield, fitness traits, and developmental features, such as leaf
162 shape, size, and complexity (Frary et al., 2000; Holtan and Hake, 2003; Fridman
163 et al., 2004; Chitwood et al., 2013; Muir et al., 2014). Comparative
164 transcriptomics for the two parents enabled identification of transcript abundance
165 variation potentially underlying trait differences between species (Koenig et al.,
166 2013). However, the genetic regulators of these transcriptional differences
167 between the species still need to be elucidated. Therefore, we used a genomics
168 approach in combination with statistical methods to identify the genetic basis of
169 transcript level variation in tomato using the *S. pennellii* introgression lines.

170 Here we report on a comprehensive transcriptome profile of the ILs, a
171 comparison between the transcript abundance patterns of the ILs and the
172 cultivated M82 background (differential gene expression – DE), as well as a
173 global eQTL analysis to identify patterns of genetic regulation of transcript
174 abundance in the tomato shoot apex. We have identified more than 7,200 *cis*-
175 and *trans*-eQTL in total, which regulate the transcript abundance of
176 approximately 5,300 genes in tomato. Additional analyses using Barnes-Hut *t*-
177 distributed stochastic neighbor embedding (BH-SNE) (van der Maaten, 2013)
178 identified 42 modules revealing novel associations between transcript abundance
179 patterns and biological processes. The transcript abundance patterns under
180 strong genetic regulation are related to plant defense, photosynthesis, and plant
181 developmental traits. We also report important eQTL regulating steady state
182 transcript abundance pattern associated with leaf number, complexity, and
183 hypocotyl length phenotypes.

184

185 **Results and Discussion**

186 **Transcriptome Profiling and Global eQTL analysis**

187 RNAseq reads obtained from the tomato shoot apex with developing
188 leaves and hypocotyl were used to identify differentially expressed (DE) genes at
189 the transcript level between each *S. pennellii* IL and the cultivated M82
190 (Supplemental Dataset 1). The total number of genes differentially expressed for
191 each IL both in *cis* (in this population reflecting “local” level regulation either from

192 within a gene itself or other genes in the introgression) and *trans*, along with the
193 number of genes in the introgression regions, are presented in Figure 1 and
194 Supplemental Table I. There was a strong correlation between the number of
195 genes in the introgression regions and the number of DE genes in *cis*
196 (Supplemental Figure S1A). In contrast, the number of DE genes in *trans* was
197 poorly correlated with introgression size (Supplemental Figure S1B). For
198 example, IL12.1.1, despite having one of the smallest introgressions, showed
199 96% of ~500 DE genes regulated in *trans* (Supplemental Table I, Supplemental
200 Figure S2). In contrast, IL1.1 and IL12.3, the ILs with highest number of genes in
201 the introgression regions, showed smaller numbers of total and *trans* DE genes
202 (Figure 1, Supplemental Table I, Supplemental Figure S2). These examples
203 suggest that specific loci and not the introgression size determine gene
204 regulation in *trans*. This could, in part, be due to the presence of genes encoding
205 key transcription factors or developmental regulators in the regions with strong
206 influence on transcript expression pattern as is seen in the *ERECTA* containing
207 genomic region in Arabidopsis (Keurentjes et al., 2007). A total of 7,943 unique
208 tomato genes were DE between the ILs and cv. M82, representing approximately
209 one third of the ~21,000 genes with sufficient sequencing depth to allow DE
210 analysis. 2,286 genes, more than one fourth of unique DE genes between the ILs
211 and cv. M82, genes showed transgressive expression patterns, i.e. those genes
212 were differentially expressed at the transcript level for the IL but not for *S.*
213 *pennellii* compared to cv. M82 (Supplemental Dataset 2 and 3). These data

214 suggest that in addition to protein coding differences, transcriptional regulation of
215 less than one third of all genes accounts for most of the phenotypic and trait
216 differences between the ILs and the cultivated parent.

217 Identifying eQTL localized to subsets of the introgressions, based on
218 overlaps between them, enabled us to narrow down the regions that contain the
219 regulatory loci. This analysis brings us one step closer to identifying potential
220 candidates that influence transcript abundance patterns in tomato. We identified
221 7,225 significant eQTL (bins) involving 5,289 unique genes across the 74 ILs
222 (Figure 2; Supplemental Dataset 4). These 7,225 significant eQTL (located in
223 bins) were designated as *cis*, *trans*, or *chromo0* (unmapped transcripts) as
224 defined in the methods and illustrated in Supplemental Figure S3, and either up
225 or down based in increase or decrease in transcript levels. This correlation
226 resulted in a total of 1,759 *cis*-up and 1,747 *cis*-down eQTL, 2,710 *trans*-up and
227 920 *trans*-down eQTL, and 51 *chromo0*-up and 38 *chromo0*-down eQTL
228 (Spearman's rho values, Supplemental Figure S4, Supplemental Table II). The
229 majority of genes (over 4,000 out of 5,289) are under the regulation of a single
230 eQTL (3,134 *cis*, 1,014 *trans*, and 19 *chromo0*; Supplemental Figure S5). This
231 observation shows the predominance of *cis*-eQTL for genetic regulation of
232 transcript abundance in the tomato ILs. Similar correlation between transcript-
233 level variation and genome-wide sequence divergence within seven Arabidopsis
234 accessions was reported to be due to *cis* control of a majority of the detected
235 variation (Kliebenstein et al., 2006).

236 The number of genes regulated by eQTL showed large variation across
237 bins. Bins on chromosomes 6, 8, and 4, such as 6B, 6C, 4D, 8A, and 8B, contain
238 predominantly *trans*-eQTL (Supplemental Dataset 5). In contrast three bins, 1F,
239 3I, and 8G, that each contains over 100 genes, have no significant *trans*- or *cis*-
240 eQTL and are transcriptionally silent. As expected, bins containing over 100
241 significant *cis*-eQTLs are scattered across the genome (Supplemental Dataset
242 5). The abundance of *trans*-eQTL on chromosomes 4, 6, and 8 strengthens the
243 idea of *trans*-eQTL hotspots controlling expression of a large number of
244 transcripts, as reported in other organisms (Brem et al., 2002; Schadt et al.,
245 2003). The resolution in this analysis is at the level of bin, and these significant
246 eQTL likely map to a smaller number of genes within the bins. Functional
247 classification of genes being regulated by these eQTL and phenotypic
248 association with the relevant ILs was undertaken to glean insights into the identity
249 of candidate genes in the bin.

250

251 **Clustering eQTL target genes into modules defined by transcript** 252 **abundance patterns**

253 In order to functionally categorize the eQTL regulated genes, Barnes-Hut
254 *t*-distributed stochastic neighbor embedding (BH-SNE, van der Maaten, 2013)
255 was performed on the 5,289 genes with eQTL to detect novel associations
256 between transcript abundance patterns. This clustering resulted in 42 distinct
257 modules containing 3,592 genes (Figure 3). Seventeen of these modules had

258 significant GO enrichment (p -value <0.05) with each module consisting of
259 transcript abundance patterns either predominately regulated by *cis*- or *trans*-
260 eQTL (Supplemental Table III). To determine which ILs are important for module
261 regulation, the median transcript abundance value of module genes for each IL
262 was calculated and used to identify ILs with significantly altered module steady
263 state transcript level.

264 Three modules were present in all mappings of the BH-SNE (van der
265 Maaten and Hinton, 2008) determined through iterations of DBscan analysis and
266 GO enrichment, and were designated as landmark modules (Figure 3B;
267 Supplemental Figure S6; Supplemental Dataset 6; Supplemental Table III). The
268 largest module had a GO enrichment for photosynthesis and related processes,
269 and significant *trans*-eQTL scattered widely across the genome with no bin or IL
270 identified as the primary regulating region (Figure 4B; Supplemental Figure S6A;
271 Supplemental Dataset 6 and 7). The second landmark module was enriched for
272 transcript abundance patterns with roles in defense, metabolism, and signaling
273 with the majority of their *trans*-eQTL mapped to IL6.2 and 6.2.2 (Figure 4A;
274 Supplemental Figure S6B; Supplemental Dataset 6 and 8). The third module,
275 which is enriched for transcript abundance patterns with cysteine-type peptidase
276 activity, was predominately composed of genes regulated by *cis*-eQTL on IL 4.2,
277 4.3, and 4.3.2 (Bins 4E and 4F) (Figure 4C; Supplemental Figure S6C;
278 Supplemental Dataset 6 and 9). A cluster of genes enriched for “peptidase
279 regulation” also emerged from a transcriptome study of leaf development for

280 three tomato species; this cluster was uniquely associated with *S. pennellii*
281 orthologs at the P5 stage of leaf development, indicating that this species has a
282 unique pattern of gene expression, which involves peptidase regulation (Ichihashi
283 et al., 2014) and may be related to leaf maturation and senescence processes
284 (Diaz-Mendoza et al., 2014).

285

286 **Genetic regulation of transcriptional responses associated with plant** 287 **defense**

288 One of the landmark modules from the clustering analysis was enriched
289 for transcript abundance patterns related to plant defense (Figure 3B;
290 Supplemental Dataset 8). Therefore we explored the genetic basis of
291 transcriptional changes associated with plant defense. IL6.2 and IL6.2.2, and
292 associated bins 6B and 6C, in particular, influence of the transcriptional
293 responses of genes associated with plant defense and signaling (Supplemental
294 Dataset 1). The genes showing increased steady-state transcript levels in both
295 ILs compared to cv. M82, as well as the genes regulated by the corresponding
296 bins, show enrichment of the GO categories response to stress and stimulus, cell
297 death, defense response, and plant-type hypersensitive response (Supplemental
298 Dataset 10 and 11). Promoter enrichment analysis for these genes showed
299 enrichment of a W-box promoter motif that is recognized by WRKY transcription
300 factors and influences plant defense response (Supplemental Dataset 12 and 13)
301 (Yu et al., 2001). Both the bins, in particular bin 6C, contain genes involved in

302 pathogen, disease, and defense response: such as *NBS-LLR resistance genes*,
303 *WRKY transcription factors*, *Multidrug resistance genes*, *Pentatricopeptide*
304 *repeat-containing genes*, *Chitinase*, and *Heat Shock Protein* coding genes. This
305 transcriptional response in the ILs is also reflected in the morphology of IL6.2.2;
306 the plants are necrotic and dwarfed (http://tgrc.ucdavis.edu/pennellii_ils.aspx,
307 Sharlach et al., 2013). Previously, a phenotypic study for the chromosome 6
308 introgression, specifically a 190Kb region in bin 6C, in a pathogen (*Xanthomonas*
309 *perforans*)/control experiment was shown to confer hypersensitive response in
310 IL6.2 and 6.2.2 (Sharlach et al., 2013). Taken together, these findings suggest
311 bins 6B and 6C contain master genetic regulators of plant defense response
312 genes, though identification of the causal gene/s that influence many other genes
313 in *trans* will need further genetic dissection of these bins.

314

315 **Genetic regulation of transcriptional responses associated with leaf** 316 **development**

317 Given the striking differences in leaf features between *Solanum pennellii*
318 and cv. M82 that are manifested in many ILs (Chitwood et al., 2013), the IL
319 population provides an excellent system for determining the extent of genetic
320 regulation of genes controlling leaf development. Previous phenotypic and QTL
321 analyses identified many ILs, such as IL4.3, IL8.1.5, IL8.1.1, and IL8.1, harboring
322 loci regulating leaf and plant developmental traits (Holtan and Hake, 2003;
323 Chitwood et al., 2013; Muir et al., 2014). IL4.3, which harbors loci with the largest

324 contribution to leaf shape and shows larger epidermal cell sizes (Chitwood et al.,
325 2013), exhibited decreased steady-state transcript levels for many genes
326 associated with cell division, such as Cyclin-dependent protein kinase regulator-
327 like protein (CYCA2;3), Cyclin A-like protein (CYCA3;1), and F-box/LRR-repeat
328 protein 2 SKP2A (Supplemental Dataset 1 and 10). In addition, genes showing
329 differences in transcript levels in IL4.3 were enriched for the promoter motifs
330 MSA (M-specific activators that are involved in M-phase specific transcription)
331 and the E2F binding site (Supplemental Dataset 11). Genes with decreased
332 transcript levels in ILs 8.1.5, 8.1.1, and 8.1, also included genes associated with
333 leaf development and morphology, genes encoding WD-40 repeat family protein
334 LEUNIG, Homeobox-leucine zipper protein PROTODERMAL FACTOR 2, and
335 the transcription factor ULTRAPETALA (Supplemental Dataset 1 and 10; Abe et
336 al., 2003; Cnops et al., 2004; Carles et al., 2005).

337 We, further, investigated the transcript expression dynamics of a set of
338 literature-curated genes related to leaf development (Ichihashi et al., 2014)
339 across the ILs and bins (Supplemental Dataset 14 and 15). A number of
340 canonical leaf developmental genes such as *SHOOT MERISTEMLESS*
341 (Solyc02g081120, *STM*), *GROWTH-REGULATING FACTOR 1* (*GRF1*,
342 Solyc04g077510), *ARGONAUTE 10* (*AGO10*, Solyc12g006790), *BELL* (*BEL1*,
343 Solyc08g081400), *LEUNIG* (Solyc05g026480) and *SAWTOOTH 1* (*SAW1*,
344 Solyc04g079830) were differentially expressed at the transcript level in more
345 than five ILs. At the level of bins, genes involved in leaf development were

346 regulated by eQTL scattered widely across the genome (Figure 4D). eQTL(bin)-
347 regulation of leaf developmental genes for some of ILs, such as IL 2.1, 4.3, 5.4,
348 8.1/8.1.1/8.1.5 and 9.1.2, showing strong leaf phenotypes is summarized in
349 Supplemental Table IV. We then examined the location of literature-curated leaf
350 developmental genes within the identified modules in the BH-SNE mapping
351 (Figure 3). The highest number of literature-curated leaf developmental genes
352 (108) was located in the photosynthesis module, whereas 19 of these genes
353 were located in the leaf development module (Supplemental Figure S7B;
354 Supplemental Dataset 16 and 17), suggesting a relationship between these two
355 modules. Over one third of the transcript expression patterns in the leaf
356 development module have significant eQTL that map to bins 4D, 8A, and 8B
357 (5.4%, 16.2%, and 15.5%, respectively; Supplemental Dataset 18), suggesting
358 that these bins contain important regulators of leaf development. This enrichment
359 of eQTL for specific bins is also consistent with the strong leaf phenotypes for ILs
360 4.3, 8.1, 8.1.1, and 8.1.5. Altogether DE, eQTL, and BH-SNE results indicate
361 that while there is no obvious master regulatory bin for leaf developmental genes,
362 many are under strong genetic regulation by eQTL distributed throughout the
363 genome (Figure 4D). This observation underscores the highly polygenic
364 regulation of leaf development (Chitwood et al., 2013) as multiple loci, residing in
365 many different chromosomal locations, regulate the expression of key leaf-
366 developmental genes at the transcriptional level.
367

368 **Genetic regulation of transcriptional responses associated with**
369 **photosynthesis**

370 Since photosynthesis GO terms were enriched for the largest module from
371 the clustering analysis (Figure 3B) and there was a correlation between
372 photosynthesis and leaf developmental modules (Supplemental Figure S7B), we
373 examined the genetic regulation of photosynthetic genes by specific ILs and
374 corresponding bins. Genes related to photosynthesis show increased transcript
375 levels across 21 ILs distributed on all chromosomes except chromosome 5
376 (Supplemental Dataset 10), showing multigenic regulation of photosynthetic
377 traits. Many of these ILs, including 8.1.5, 8.1.1, 8.1 and 4.3, and associated bins
378 showed regulation of genes linked to photosynthesis, chlorophyll biosynthesis,
379 and response to light stimulus (Supplemental Dataset 10 and 11). This
380 observation indicates that ILs may also differ from each other and from the
381 cultivated M82 background in photosynthetic efficiency. However no studies, so
382 far, have investigated the photosynthetic phenotype of these ILs.

383 To analyze the relationship between the leaf development and
384 photosynthesis modules the median transcript abundance value of all genes in
385 each module was compared resulting in a significant negative correlation ($\text{adj } r^2$
386 = 0.77; Figure 5). This analysis likely reflects the transition from leaf development
387 to leaf maturation captured in our shoot meristem samples. The genes found in
388 the leaf development module may promote developmental processes such as
389 cell division and maintenance or meristematic potential, whereas the leaf

390 development related genes found in the photosynthesis module may act to
391 suppress this process to allow for maturation of the leaf. The two modules had
392 their most influential eQTL on bins 4D, 8A, and 8B (Supplemental Dataset 6;
393 Supplemental Figure S7A), suggesting that leaf development and photosynthetic
394 genes not only have transcript levels in opposition but also likely share common
395 regulatory loci. This finding is consistent with the link between leaf development
396 and photosynthesis that we established previously by meta-analysis of
397 developmental and metabolic traits (Chitwood et al., 2013).

398

399 **Dissection of identified eQTL to spatially- and temporally- regulated** 400 **development**

401 Since the eQTL study used shoot apices that includes the shoot apical
402 meristem (SAM) and developing leaves, we resolved the detected eQTL to
403 specific tissues and temporally-regulated development using previous gene
404 expression data. We analyzed transcript abundance in laser micro-dissected
405 samples representing the shoot apical meristem (SAM) + P0 (the incipient leaf)
406 vs. the P1 (the first emerged leaf primordium) that represents transcript levels in
407 the meristem (SAM) and the first differentiated leaf (P1) (Figure 6A). We also
408 analyzed hand dissected samples of the SAM + P0-P4 vs. the P5 collected over
409 time (Figure 6B-C), representing genes regulated by vegetative phase change
410 (heteroblasty) (Chitwood et al., 2015).

411 Using a bootstrapping approach, we identified bins statistically enriched
412 for genetically regulating genes with previously identified transcript expression
413 patterns (Figure 6D-F). Except for one instance (cis-regulated genes with high
414 SAM/P0 expression located in bin 2I), bins enriched for transcript expression
415 patterns represented *trans* regulation, hinting at predominant regulation of gene
416 expression patterns mediated by transcription factors at the level of transcription.
417 Most SAM/P0 vs. P1 enriched bins were enriched for P1 transcript expression
418 (Figure 6D). We previously showed that genes with high P1 transcript levels are
419 enriched for photosynthetic-related GO terms, compared to SAM/P0 genes
420 enriched for transcription, cell division, and epigenetics-related GO terms
421 (Chitwood et al., 2015), suggesting a genetic basis at both a functional and
422 tissue-specific level for genes related to photosynthesis expressed preferentially
423 in the P1 compared to the SAM/P0.

424 Bins enriched for regulation of genes with temporally-dependent steady
425 state transcript levels were mostly associated with genes with decreasing
426 transcript level over time, for both the SAM + P0-P4 and P5 (Figure 6E-F).
427 Interestingly, 3 bins (7E, 7F, and 8A) share enrichment for genes with decreasing
428 transcript levels over time in both the SAM + P0-P4 and P5 (Figure 6E-F),
429 suggesting true temporal *trans* regulation, regardless of tissue, by these loci.
430 Broadly, genes with increasing transcript levels over time are associated with
431 transcription and small RNA GO terms in both the SAM + P0-P4 and P5,
432 whereas decreasing transcript levels over time is associated with translation

433 associated GO terms in the SAM + P0-P4 and photosynthetic activity in the P5
434 (Supplemental Dataset 19).

435

436 **Linking leaf and hypocotyl phenotypes to detected eQTL**

437 In order to connect detected eQTL with leaf and hypocotyl phenotypes
438 under two different environmental conditions, we correlated transcript abundance
439 with leaf number, leaf complexity (as measured in Chitwood et al., 2014), and
440 hypocotyl length phenotypes of the ILs grown under simulated sun and shade
441 conditions. Significant correlations with transcript abundance patterns were
442 identified for all three phenotypes analyzed under both treatments (Supplemental
443 Table V). Focusing on a subset of these transcript expression patterns that had
444 associated eQTL enabled us to connect the phenotypes to their regulatory loci
445 (Supplemental Table V).

446 Genes negatively correlated with leaf number showed enrichment of leaf
447 development GO terms, whereas positively correlated genes showed enrichment
448 of photosynthesis-related GO terms (Supplemental Figure S8A-B; Supplemental
449 Dataset 2 in Chitwood et al., 2014). For the leaf complexity trait, correlations
450 were reversed compared to leaf number (Supplemental Figure S9A-B;
451 Supplemental Dataset 20). The transcript levels of these genes associated with
452 leaf number were predominantly regulated by eQTL on chromosomes 7 and 8
453 (Supplemental Figure S8C-D), and those of leaf complexity on chromosomes 4,
454 7, and 8 (Supplemental Figure S9C-D). These results, in combination with DE,

455 eQTL, and BH-SNE, highlight bins on chromosomes 4 and 8 as important genetic
456 regulators of leaf developmental genes.

457 Five genes were positively correlated with hypocotyl length under
458 simulated shade and one gene (Solyc10g005120) was negatively correlated with
459 hypocotyl length under both sun and shade (Figure 7A; Supplemental Dataset
460 21). eQTL for the positively correlated genes are located on chromosomes 3, 7,
461 and 11, whereas the single cis-eQTL for the negatively correlated gene,
462 Solyc10g005120 (an uncharacterized *Flavanone 3-hydroxylase-like* gene), was
463 located in bin 10A.1 (Supplemental Figure S10; Figure 7B). The transcript is only
464 expressed in IL 10.1, which has the *S. pennellii* version of the gene and an
465 attenuated shade avoidance response, but is not expressed in IL 10.1.1, which
466 has the M82 version of the gene and a normal shade avoidance response
467 (Supplemental Figure S11). This indicates that genes in bin 10A, the non-
468 overlapping regions of 10.1 and 10.1.1, are responsible for the shade avoidance
469 response. Bin 10A includes Solyc10g005120, the one gene negatively correlated
470 with hypocotyl length under both sun and shade. .

471 A set of BILs (Backcross Inbred Lines), developed from cv. M82 and *S.*
472 *pennellii*, provide higher resolution gene mapping with smaller bin sizes (Muller et
473 al., 2016; Fulop et al., 2016). To further explore the role of Solyc10g005120 we
474 used BIL-128, which contains a sub-region of bin 10A and has a secondary
475 introgression on chromosome 2 (Supplemental Figure S10). Influence of the
476 secondary introgression was examined using BIL-033, which-shares the

477 introgression on chromosome 2. BIL-128 has an attenuated shade avoidance
478 response, as does 10.1, whereas BIL-033 undergoes a shade avoidance
479 response similar to that of cv. M82 (Supplemental Figure S11). These results rule
480 out the influence of chromosome 2 genes on the attenuated hypocotyl phenotype
481 and confirm the influence of the bin 10A sub-region, which includes
482 Solyc10g005120, on the attenuated hypocotyl phenotype (Supplemental Figure
483 S10; S11). Solyc10g005120 is an uncharacterized gene and our observations
484 highlight it as a new candidate regulating shade avoidance responses.

485

486 **Conclusion**

487 In this study we have investigated the regulation of steady state transcript
488 levels in the progeny of crosses between cultivated tomato (*Solanum*
489 *lycopersicum* cv. M82) and a wild relative (*Solanum pennellii*). A combination of
490 differential gene expression, eQTL, and clustering analyses provide a
491 comprehensive picture of genetic regulation of transcript expression patterns in
492 this IL population. Our data show that some biological pathways, such as plant
493 defense, are under the regulation of a limited number of loci with strong effects,
494 whereas loci regulating other pathways, such as photosynthesis and leaf
495 development, are scattered throughout the genome most likely with weaker
496 individual effects. We correlated transcript levels with leaf and hypocotyl
497 phenotypes and identified the regulatory regions driving these transcript
498 expression patterns. Coupled with comprehensive phenotyping on these ILs,

499 these data set provide a valuable resource to design strategies to achieve a
500 desirable plant phenotype through genetic manipulation of the transcript
501 abundance of key genes or gene modules. Our ability to predict and understand
502 the downstream effects of genes introgressed from wild relatives on gene
503 expression patterns and ultimately phenotypes will be a critical component of
504 crop plant enhancement.

505

506 **Materials and Methods**

507 **Plant Materials, Growth Conditions, and Experimental Design**

508 Plant materials, growth conditions, and experimental design were described in
509 (Chitwood et al., 2013), but are outlined here briefly. Seeds of *Solanum pennellii*
510 ILs (Eshed and Zamir, 1995; Liu and Zamir, 1999) and *Solanum lycopersicum* cv.
511 M82 were obtained either from Dani Zamir (Hebrew University, Rehovot, Israel)
512 or from the Tomato Genetics Resource Center (University of California, Davis).
513 Seeds were stratified in 50% bleach for 2 min., grown in darkness for 3 d for
514 uniform germination before moving to a growth chambers for 5 days. Six
515 seedlings of each genotype were planted per pot for each replicate. The 76 ILs
516 (and two replicates each of cv. M82 and *S. pennellii*) were divided into four
517 cohorts of 20 randomly assigned genotypes. These cohorts were placed across
518 four temporal replicates in a Latin square design as described in (Chitwood et al.,
519 2013). The seedlings were harvested 5 d after transplanting (13 d of growth in
520 total). Cotyledons and mature leaves >1 cm in total length were excluded, and

521 remaining tissues (including the shoot apical meristem) above the midpoint of the
522 hypocotyl were pooled, for all individuals in a pot, into 2-mL microcentrifuge tubes
523 and immediately frozen in liquid nitrogen. Two ILs, IL7.4 and IL12.4.1 were not
524 included in the final analysis due to seed contaminations.

525

526 **Growth conditions and quantification of hypocotyl length**

527 Seeds 76 ILs (covering the entire genome) along with the parents were
528 sterilized using 70% ethanol, followed by 50% bleach, and finally rinsed with
529 sterile water. This experiment was replicated three times each in 2011 and 2012.
530 Ten to twelve seeds of each IL were sown into Phytatray II (Sigma-Aldrich)
531 containers with 0.5x Murashige and Skoog minimal salt agar. Trays were
532 randomized and seeds germinated in total darkness at room temperature for 48h.
533 Trays of each IL were randomly assigned to either a sun or shade treatment
534 consisting of 110 μ Mol PAR with a red to far-red ratio of either 1.5 (simulated sun)
535 or 0.5 (simulated shade) at 22°C with 16 hour light / 8 hour dark cycles for 10d.
536 Three genotypes were excluded from the analyses due to poor germination
537 (IL3.3) or their necrotic dwarf phenotypes (IL6.2, 6.2.2). After 10d, seedlings were
538 removed from the agar and placed onto transparency sheets containing a
539 moistened kimwipe to prevent dehydration and scanned using an Epson V700 at
540 8-bit grayscale at 600 dpi. Image analysis was carried out using the software
541 ImageJ (Abramoff et al., 2004).

542 For hypocotyl length analysis of backcross inbred lines between *S.*
543 *pennellii* and *S. lycopersicum* cv. M82, seeds were sterilized in 50% bleach and
544 then rinsed with sterile water. The seeds were then placed in Phytatrays in total
545 dark at room temperature for 72 hours, and then moved to 16 hour light / 8 hour
546 dark for 4d. Seedlings were transferred to soil using a randomized design and
547 assigned to either a sun or shade treatment (as described above) for seven days.
548 Images were taken with a HTC One M8 Dual 4MP camera and hypocotyl lengths
549 measured in ImageJ (Abramoff et al., 2004) using the Simple Neurite Tracer
550 (Longair et al., 2011) plugin.

551

552 **RNA-Seq Library Preparation and Preprocessing RNA-Seq Sequence Data**

553 RNAseq libraries were prepared and the reads were preprocessed as described
554 in (Chitwood et al., 2013), and are outlined here. mRNA isolation and RNA-Seq
555 library preparation were performed from 80 samples at a time using a high-
556 throughput RNA-Seq protocol (Kumar et al., 2012). The prepared libraries were
557 sequenced in pools of 12 for replicates 1 and 2 (one lane each) and in pools of
558 80 for replicates 3 and 4 (seven lanes) at the UC Davis Genome Centre
559 Expression Analysis Core using the HiSeq 2000 platform (Illumina).
560 Preprocessing of reads involved removal of low quality reads (phred score < 20),
561 trimming of low-quality bases from the 39 ends of the reads, and removal of
562 adapter contamination using custom Perl scripts. The quality-filtered reads were
563 sorted into individual libraries based on barcodes and then barcodes were

564 trimmed using custom Perl script.

565

566 **Read Mapping and Quantification of Transcript Levels**

567 Mapping and normalization were done on the iPLANT Atmosphere cloud server

568 (Goff et al., 2011). *S. lycopersicum* reads were mapped to 34,727 tomato cDNA

569 sequences predicted from the gene models from the ITAG2.4 genome build

570 (downloadable from

571 ftp://ftp.solgenomics.net/tomato_genome/annotation/ITAG2.4_release/). A

572 pseudo reference list was constructed for *S. pennellii* using the homologous

573 regions between *S. pennellii* scaffolds v.1.9 and *S. lycopersicum* cDNA

574 references above. Using the defined boundaries of ILs, custom R scripts were

575 used to prepare IL-specific references that had the *S. pennellii* sequences in the

576 introgressed region and *S. lycopersicum* sequences outside the introgressed

577 region. The reads were mapped using BWA (Li and Durbin, 2009; Roberts and

578 Pachter, 2013) using default parameters except for the following that were

579 changed: `bwa aln: -k 1 -l 25 -e 15 -i 10` and `bwa samse: -n 0`. The bam alignment

580 files were used as inputs for `express` software to account for reads mapped to

581 multiple locations (Roberts and Pachter, 2013). The estimated read counts

582 obtained for each gene for each sample from `express` were treated as raw counts

583 for differential gene expression analysis. The counts were then filtered in R using

584 the Bioconductor package `EdgeR` version 2.6.10 (Robinson and Oshlack, 2010)

585 such that only genes that had more than two reads per million in at least three of

586 the samples were kept. Normalization of read counts was performed using the
587 trimmed mean of M-values method (Robinson and Oshlack, 2010), and
588 normalized read counts were used to identify genes that are differentially
589 expressed at the transcript level in each IL compared to cv. M82 parent as well
590 as in between two parents, *S. pennellii* and M82. The DE genes for each IL were
591 compared to those between the two parents to identify genes that were
592 differentially expressed for the IL but not for *S. pennellii* compared to cv. M82.
593 Those genes were considered to show transgressive expression pattern at the
594 transcript level for the specific IL, whereas other DE genes were considered to
595 show the transcript expression similar to *S. pennellii*.

596

597 **Correlation of phenotype with pattern of steady state transcript levels**

598 Transcript level patterns were correlated with three phenotypes collected
599 from the ILs along with the parents. Normalized estimated read counts with 3-4
600 independent replicates per IL were log₂ transformed prior to the analyses. Leaf
601 number and leaf complexity were collected from the ILs as outlined in Chitwood
602 et al. (2014) under both sun and shade treatments. Hypocotyl lengths were
603 measured as detailed above. To test whether the transcript level for a given gene
604 was correlated with a particular phenotype, bootstrapping analyses were
605 performed. Transcript levels and phenotype data were randomly permuted (with
606 replacement) using the sample() function against IL and then merged. For each
607 analysis, 1000 replications were performed and the p-values were calculated

608 from the Spearman's rho value distributions. P-values were adjusted for multiple
609 comparisons using the BH correction (Benjamini & Hochberg, 1995). Significant
610 correlations were identified as those with an adjusted p-value < 0.05 and the
611 mean rho value (the correlation coefficient) was used to designate the correlation
612 as either positive (positive slope) or negative (negative slope). All analyses were
613 implemented using the statistical software R and custom scripts (R Core Team,
614 2015).

615

616 **Methods for eQTL Analyses**

617 eQTL mapping analyses were performed to determine whether the transcript
618 level of a gene is correlated with the presence of a specific introgression from *S.*
619 *pennellii* into *S. lycopersicum* cv. M82. This correlation was examined at the level
620 of "bin", with a bin defined as a unique overlapping region between
621 introgressions. Examining eQTL at the bin level enables those eQTL to be
622 mapped to considerably smaller intervals than the ILs themselves (Liu and Zamir,
623 1999). eQTL mapping analyses were performed on the normalized estimated
624 read counts with 3-4 independent replicates per IL, which were log2 transformed
625 prior to the analyses. To test whether the transcript level for a given gene is
626 correlated with the presence of a particular bin, a Spearman's rank correlation
627 test was used with ties resolved using the midrank method. P-values were
628 adjusted for multiple comparisons using the BH correction (Benjamini and
629 Hochberg, 1995). Significant eQTL were identified as those with an adjusted p-

630 value < 0.05 and Spearman's rho (the correlation coefficient) was used to
631 designate the eQTL as up (positive slope) or down (negative slope). Significant
632 eQTL were also designated as *cis* (defined as local gene regulation within the
633 same bin) - if the gene was located on the bin with which it is correlated, *trans*
634 (distant) - if the gene was correlated with a bin that is neither the bin it is on nor a
635 bin that shares an overlapping IL with the correlated bin, or *chromo0* - if the gene
636 lies in the unassembled part of the genome. When a gene has a designation *cis*-
637 eQTL, and a secondary correlation was found with a bin that shares an
638 overlapping introgression, this secondary correlation was not designated as an
639 eQTL. When a gene does not have a designated *cis*-eQTL and a correlation was
640 found with a bin that shares an overlapping introgression, this correlation was
641 designated as a *trans*-eQTL. All analyses were implemented using the statistical
642 software R and custom scripts (R Core Team, 2015).

643

644 **Methods for eQTL clustering analysis**

645 **Data Preparation:** In preparation for analysis using the Barnes-Hut-SNE
646 algorithm, the data set was log₂ transformed. The transcript level for each gene
647 was then normalized across all 74 introgression lines so that the profile had a
648 mean of zero and a standard deviation of one. Normalization of the data allowed
649 for comparison of the relative relationship between each gene expression profile
650 (Bushati et al., 2011).

651 **Barnes-Hut-SNE:** t -SNE or t -distributed stochastic neighbor embedding (van
652 der Maaten and Hinton, 2008) is a non-linear dimensionality reduction method,
653 which faithfully maps objects in high dimensional space (H-space) into low
654 dimensional space (V-space). Crowding is avoided through the long-tailed t -
655 distribution, which forces non-neighbor clusters farther away from each other in
656 V-space than those clusters actually are in H-space (van der Maaten and Hinton,
657 2008). The exaggerated separation of non-neighboring clusters improves 2D
658 resolution, allowing identification of novel groupings not readily apparent in other
659 clustering methods. However this method is resource intensive, and with higher
660 dimensionality, the number of genes that can be analyzed is limited. We have
661 used Barnes-Hut-SNE, a newer implementation of t -SNE that greatly increases
662 the speed and number of genes that can be analyzed, for the present analysis
663 (van der Maaten, 2013). Barnes-Hut-SNE accomplishes this efficiency through
664 the use of a Vantage Point tree and a variant of the Barnes-Hut algorithm (van
665 der Maaten, 2013). For clustering, 2D maps were generated using a perplexity of
666 30 and without the initial PCA step from the Barnes-Hut-SNE R implementation
667 (Rtsne package; Krijthe, 2014). Theta was set to 0.3 based on (van der Maaten,
668 2013) in order to maintain an accurate dimensionality reduction without
669 sacrificing processing speed.

670 **Clustering for Module Selection:** The DBscan algorithm (Density Based spatial
671 clustering of applications with noise) was used to select modules from the
672 Barnes-Hut-SNE results (fpc package; Hennig, 2014). This algorithm had the

673 advantage of both selecting modules and removing any genes that fell between
674 modules. The scanning range (*epsilon*) and minimum seed points (*minpts*) were
675 selected manually, and used to determine if any one point is a member of a
676 cluster based on physical positioning within the mapping relative to neighboring
677 points. A *minpts* of 25 was used to capture smaller modules on the periphery and
678 an *epsilon* of 2.25 was used to avoid the overlapping of internal and closely
679 spaced modules.

680 **Plots:** Boxplots were generated from normalized transcript abundance values for
681 each module. The ribbon plot was generated from correlated abundance values
682 from leaf development and photosynthesis related modules. These plots were
683 generated using ggplot from the ggplot2 R Package (Wickham, 2009). The
684 median transcript levels of the genes mapped to a module was calculated for
685 each IL and replicated for all modules. Significant ILs were identified as those
686 with a median transcript level greater than 1 standard deviation from the mean of
687 all genes across all ILs in the module.

688

689 **GO Enrichment analysis**

690 Differentially expressed genes at the transcript level for individual ILs and genes
691 with significant eQTL were analyzed for enrichment of Gene Ontology (GO)
692 terms at a 0.05 false discovery rate cutoff (goseq Bioconductor package; Young
693 et al., 2010).

694

695 **Promoter enrichment analysis**

696 Promoter enrichment analysis was performed by analyzing the 1000 bp upstream
697 of the ATG translational start site for genes with significant eQTL using 100
698 motifs represented in the AGRIS AtTFDB (<http://arabidopsis.med.ohio->
699 [state.edu/AtTFDB](http://arabidopsis.med.ohio-state.edu/AtTFDB)). The Biostrings package was used to analyze the abundance
700 of 100 motifs in groups of genes with significant eQTL compared to motif
701 abundance in promoters of all analyzed genes using a Fisher's exact test ($p <$
702 0.05) with either zero or one mismatch (Ichihashi et al., 2014).

703

704 **Dissection of eQTL to different stages and time of development at shoot**
705 **apex**

706 Differentially expressed genes with enriched transcript levels in laser micro-
707 dissected SAM/P0 vs. P1 samples or hand-dissected samples of the SAM + P0-
708 P4 or P5 sampled over developmental time were obtained from Chitwood et al.,
709 2015. Genes for which a differential expression call could be made (i.e., had
710 enough reads and passed quality filters) were merged with detected eQTL using
711 the `merge()` function in R (R Core Team, 2015). For bootstrapping, *cis*- and *trans*-
712 regulated transcripts were analyzed separately. Merged transcript abundance
713 patterns were randomly permuted (without replacement) using the `sample()`
714 function against bin identity. For each test, 10,000 permutations were sampled to
715 count the times that a particular transcript expression pattern was assigned to a
716 bin more than the actual count. Resulting frequencies, representing a probability

717 value, were multiple test adjusted using the Benjamini-Hochberg (Benjamini and
718 Hochberg, 1995) method using `p.adjust()`. Those bins with multiple test adjusted
719 probability values <0.05 were analyzed further using visualizations created with
720 `ggplot2` (Wickham, 2009).

721

722 **Sequence submission**

723 The quality filtered, barcode-sorted and trimmed short read dataset, which was
724 used to get the normalized read counts and for differential gene expression
725 analysis, was deposited to the NCBI Short Read Archive under accessions
726 SRR1013035 - SRR1013343 (Bioproject accession SRP031491).

727

728 **Supplemental files**

729

730 **Supplemental figures:**

731 **Supplemental Figure S1. Number of genes in the introgression region for**
732 **an IL and the number of differentially expressed genes at the transcript**
733 **level compared to cv. M82.** Strong correlation was observed for differentially
734 expressed genes in *cis* (A), whereas a weak correlation was observed for genes
735 in *trans* (B).

736

737 **Supplemental Figure S2. Histograms for differentially expressed genes at**
738 **the transcript level for the ILs.** Genes with increased or decreased transcript
739 levels for the ILs in *cis* (A), and in *trans* (B).

740

741 **Supplemental Figure S3. eQTL and the transcript abundance patterns they**
742 **regulate.** Each blue bar is a unique introgression. When the transcript
743 abundance pattern of gene 1 is correlated with bin-A, then bin-A contains a *cis*-
744 eQTL. When the transcript abundance pattern of gene 1 is correlated with bin-E
745 then bin-E contains a *trans*-eQTL. When gene 2 has a *cis*-eQTL designated for
746 bin-D and the transcript abundance pattern of gene 2 is also correlated with bin-
747 B, then this secondary correlation is not designated as an eQTL, since these bins
748 share overlapping introgression regions. When the transcript abundance pattern
749 of gene 2 is correlated with bin-B and gene 2 does not have a *cis*-eQTL
750 designated for bin-D, then bin-B is designated as a *trans*-eQTL. All eQTLs for
751 genes that lie in the unassembled portion of the genome (not on any
752 chromosome) cannot be designated as either *cis* or *trans* and are designated
753 *chromo0*-eQTL.

754

755 **Supplemental Figure S4. *Cis*- and *Trans*-eQTL.** Histograms plotting the
756 numbers of significant eQTL mapped to each bin across the 12 chromosomes of
757 *S. lycopersicum* (M82). A. *cis*-eQTLs. B. *trans*-eQTLs.

758

759 **Supplemental Figure S5. Frequency and distribution of differentially**
760 **expressed genes at the transcript level for the IL population at the**
761 **introgression and the bin level.** (A) Frequency of genes differentially expressed

762 in one or more ILs. (B) Frequency of genes being regulated by one or more
763 BINs/eQTL.

764

765 **Supplemental Figure S6. Boxplots of the normalized transcript levels for**
766 **the three landmark modules.** The relative transcript levels of all genes found in
767 each module for the 74 ILs. The y-axis is the relative transcript level of all eQTL
768 for each IL. (A) Photosynthesis module. (B) Defense, metabolism, and signaling
769 module. (C) Cysteine-type peptidase activity module. Asterisks represent ILs with
770 a median transcript level significantly different from the module mean.

771

772 **Supplemental Figure S7. Normalized transcript levels of the leaf**
773 **development module and genes associated with leaf development within**
774 **the mapping.** (A) Boxplot of normalized transcript level for the leaf development
775 module. The 108 genes contained in the leaf development module and their
776 relative median transcript level for each IL. Asterisks represent ILs with a median
777 transcript levels significantly different from the module mean. (B) Literature-
778 curated genes related to leaf development (Ichihashi et al., 2014) overlaid on the
779 Leaf Development and Photosynthesis modules. False colored orange, dark
780 blue, and light blue respectively.

781

782 **Supplemental Figure S8. eQTL regulation of transcript abundance patterns**
783 **that correlate with leaf number.**

784 A, B) Forty-two distinct modules identified by DBscan from the eQTL mapping
785 generated by BH-SNE analysis. Modules enriched for genes with leaf
786 development and photosynthesis GO terms are labeled in blue and green,
787 respectively. Genes with transcript levels correlated with leaf number under
788 simulated sun (A) and shade (B) are indicated by squares with positive
789 correlations in red and negative correlations in yellow.

790 C, D) Genes with transcript levels correlated with leaf number under simulated
791 sun (C) and shade (D) are shown connected to their respective eQTL with
792 chords. I) The 12 tomato chromosomes in megabases. II) Colored boxes indicate
793 the sizes of each bin. III) Black bars indicate the locations of the genes. IV)
794 Chords connect eQTL to the genes whose transcript levels they regulate. Chords
795 are colored by the chromosome location of the eQTL.

796

797 **Supplemental Figure S9. eQTL regulation of transcript abundance patterns**
798 **that correlate with leaf complexity.**

799 A, B) Forty-two distinct modules identified by DBscan from the eQTL mapping
800 generated by BH-SNE analysis. Modules enriched for genes with leaf
801 development and photosynthesis GO terms are labeled in blue and green,
802 respectively. Genes with transcript levels correlated with leaf complexity under
803 simulated sun (A) and shade (B) are indicated by squares with positive
804 correlations in red and negative correlations in yellow.

805 C, D) Genes with transcript levels correlated with leaf complexity under simulated
806 sun (C) and shade (D) are shown connected to their respective eQTL with
807 chords. I) The 12 tomato chromosomes in megabases. II) Colored boxes indicate
808 the sizes of each bin. III) Black bars indicate the locations of the genes. IV)
809 Chords connect eQTL to the genes whose transcript levels they regulate. Chords
810 are colored by the chromosome location of the eQTL.

811

812 **Supplemental Figure S10. Distributions of introgressions from *S. pennellii***
813 **into *S. lycopersicum* cv. M82.** Map of chromosomes 2, 10, and 11 showing the
814 locations of the introgressions for BIL 033 and 128, as well as the overlapping IL
815 regions, which define the bind (Modified from Chitwood et al., 2013).

816

817 **Supplemental Figure S11. Tomato hypocotyl length under sun and shade**
818 **treatments.** M82 shows a typical shade response with a significantly longer
819 hypocotyl in the shade (Δ of 7 mm). IL 10.1 and BIL 128, which share an
820 overlapping introgression (**Supplemental Fig. S10**), do not significantly respond
821 to the shade treatments. The presence of a response in BIL 033 in combination
822 with the shared introgression with BIL 128 on chromosome 2, indicates that the
823 gene region responsible for the lack of shade response in BIL 128 is located in
824 the introgression on chromosome 10. Bars represent means \pm SE with a
825 minimal of $N = 22$ for each (ANOVA, $F_{7,182} = 44.6$, $p < 0.001$). Letters indicate
826 differences at the $p < 0.05$ significance level for Tukey pairwise tests.

827

828 **Supplemental tables:**

829 **Supplemental Table I. Number of differentially expressed (DE) genes at the**
830 **transcript level in *cis*, *trans*, and the total number of DE genes for the ILs**
831 **along with number of genes in the introgression region.**

832

833 **Supplemental Table II. Correlation coefficients (Spearman's rho) for**
834 **significant eQTLs.** The significant eQTL are classified into *trans*, *cis*, and
835 *chromo0*, then designated as up (positive slope) or down (negative slope) based
836 on the correlation coefficients.

837

838 **Supplemental Table III. GO enrichment and *cis* or *trans* regulation of the 42**
839 **identified modules.** All 42 distinct modules are listed with the total number of
840 genes present in each module. The GO enrichment (if one is present) is given
841 for each module, along with whether that module is predominantly *cis* or *trans*
842 regulated. Only nine of the forty-two module show *trans* correlation, which
843 includes the leaf development module.

844

845 **Supplemental Table IV. Leaf developmental phenotypes of selected ILs and**
846 **genetic effects of eQTL (bin) on transcript levels of candidate genes.** Some
847 of the ILs with strong leaf phenotypes are listed along with the associated

848 regulatory QTL (bin) that regulate the transcript levels of candidate leaf-
849 developmental genes.

850

851 **Supplemental Table V. Significant correlations between transcript**
852 **expression patterns and phenotypes.** Bootstrapping analyses correlated
853 transcript expression patterns across the 74 ILs with three phenotypes in under
854 both sun and shade treatments. Genes with significant correlations that also have
855 eQTL are listed.

856

857 **Supplemental datasets:**

858 **Supplemental Dataset 1. List of Differentially Expressed Genes at the**
859 **transcript level.** List of significant (FDR < 0.05) differentially expressed genes
860 for each Introgression line (IL) compared to cultivated parent *Solanum*
861 *lycopersicum* cv. M82. For each IL, gene ID, log Fold Change (logFC), log
862 Counts Per Million (logCPM), P-value, False Discovery Rate (FDR) as well as
863 annotation of the differentially expressed genes are presented. The differentially
864 expressed genes for each IL are listed on separate sheets of the file as
865 mentioned on the label of each sheet.

866

867 **Supplemental Dataset 2. Transgressive expression of genes at the**
868 **transcript level among ILs.** Detailed results on transgressive transcript levels of

869 genes for the IL population is presented along with the relevant diagrams and
870 enriched GO-categories for the genes showing transgressive transcript level.

871

872 **Supplemental Dataset 3. Genes with Transgressive transcript level.** List of
873 the genes showing transgressive transcript level in the IL population along with
874 details of their transcript abundance and annotation.

875

876 **Supplemental Dataset 4. . All genes with significant eQTL.** Gene locations
877 are specified by columns: chromosome, bin, binIL.code1-4, begin, end, and
878 sort.order. eQTL bin locations are specified by columns: cor.bin, cor.bin.ILcode1-
879 4, and bin.order. eQTL statistics are in columns: slope.rho.spearman,
880 pvalue.spearman, BHpvalue.spearman, up.down, and cis.trans. AGI and ITAG
881 annotations are listed for the genes in columns V-Y.

882

883 **Supplemental Dataset 5. Number of eQTL and genes per bin.** Numbers of
884 *trans*-, *cis*-, and *chromo0*-eQTL are reported for each bin and per gene within
885 each bin.

886

887 **Supplemental Dataset 6. Number of eQTL and the bin on which those eQTL**
888 **reside for each of the landmark modules and Leaf Development**
889 **module.** The Photosynthesis, Defense, Cysteine-Type Peptidase Activity and
890 Leaf Development modules are listed with the bins on which their eQTL reside.

891 The number eQTL per bin and the percentage of total eQTL within each module
892 are listed.

893

894 **Supplemental Dataset 7. Photosynthesis module gene list.** Gene ID of all
895 genes within the Photosynthesis module with description.

896

897 **Supplemental Dataset 8. Defense module gene list.** Gene ID of all genes
898 within the Defense, Metabolism and Signaling module with description.

899

900 **Supplemental Dataset 9. Cysteine-type module gene list.** Gene ID of all
901 genes within the Cysteine-type Peptidase module with description.

902

903 **Supplemental Dataset 10. GO Enrichment for DE Genes.** Enriched GO and
904 GOslim categories for the genes with increased and decreased transcript levels
905 in each IL compared to cultivated parent *Solanum lycopersicum* cv. M82.

906

907 **Supplemental Dataset 11. GO Enrichment for eQTL.** Enriched GO and
908 GOslim categories for all the eQTL mapped to a bin, as well as the *cis*- and
909 *trans*-eQTL separately.

910

911 **Supplemental Dataset 12. Promoter Motif Enrichment for DE Genes.**

912 Enriched promoter motifs with no mismatch for the up- and down-regulated
913 genes in each IL compared to cultivated parent *Solanum lycopersicum* cv. M82
914 are shown along with the p-value for significance.

915

916 **Supplemental Dataset 13. Promoter Motif Enrichment for *trans*-eQTL.** eQTL
917 are grouped by bin (cor.bin) and promoters were analyzed for both zero and one
918 mismatch with p-values for each. Bins can be ordered using the column,
919 bin.order.

920

921 **Supplemental Dataset 14. Differentially expressed leaf Developmental**
922 **Genes at the transcript level.** Frequency of differentially expressed literature-
923 curated leaf-developmental genes among the ILs. Genes that show differential
924 transcript level in at least one IL are listed. Genes, chromosomes, annotation and
925 the number of ILs showing differential transcript level of the genes are listed

926

927 **Supplemental Dataset 15. Curated list of leaf developmental genes with**
928 **eQTLs.** Gene locations are specified by columns: chromosome, bin, binIL.code1-
929 4, begin, and end. eQTL bin locations are specified by columns: cor.bin, and
930 cor.bin.ILcode1-4. eQTL statistics are in columns: slope.rho.spearman,
931 pvalue.spearman, BHpvalue.spearman, up.down, and cis.trans. AGI annotations
932 for the genes are in columns: Arabidopsis_orthologue and Gene_name.

933 **Supplemental Dataset 16. Literature-curated plus list of leaf development**
934 **genes present in the leaf development modules.** Nineteen genes from the
935 literature-curated plus list (Ichihashi et al., 2014) were present within the leaf
936 development module, representing approximately 3% of the curated genes and
937 11% of the curated genes found in the eQTL data set. The Gene ID, *Arabidopsis*
938 orthologue, and a description for each gene is provided.

939

940 **Supplemental Dataset 17. Literature-curated plus list of leaf development**
941 **genes that are present in all modules.** A total of 175 genes from the curated
942 list plus of leaf developmental genes (Ichihashi et al., 2014) were present in the
943 5,289 genes with significant eQTL. Matching gene number is the number of
944 genes in the module, which were found in the curated list. The percent of curated
945 genes defines the percentage of matched genes in a module out of the total
946 curated list plus. The percent total in eQTL represents the percentage of matched
947 genes in a module out of the 175 present only in the eQTL. The Photosynthesis
948 and leaf development modules contain the highest proportion of leaf
949 development curated genes.

950

951 **Supplemental Dataset 18. Leaf Development module gene list.** Gene ID of all
952 genes within the Leaf Development module with description.

953

954 **Supplemental Dataset 19: GO enrichment for bins statistically enriched for**
955 **transcripts expressed spatio-temporally across tissues.** Enriched GO and
956 GOslim categories for all transcripts expressed spatio-temporally across tissues
957 and with *trans*-eQTL residing in a bin.

958

959 **Supplemental Dataset 20: Leaf complexity phenotype of ILs.** Total leaf
960 complexity data for all the ILs under simulated sun and shade is listed.

961

962 **Supplemental Dataset 21: Hypocotyl phenotype of ILs.** Hypocotyl length data
963 for all the ILs under simulated sun and shade for two years is listed.

964

965 **Acknowledgments**

966 We thank Lauren R. Headland, Jason Kao and Paradee Thammapijai for help
967 in generating plant materials. We also thank Mike Covington for his advice on
968 bioinformatic analyses. We thank the Vincent J. Coates Genomics Sequencing
969 Laboratory at UC Berkeley (supported by NIH S10 Instrumentation Grants
970 S10RR029668 and S10RR027303), and computational resources/cyber
971 infrastructure provided by the iPlant Collaborative (www.iplantcollaborative.org),
972 funded by the National Science Foundation (Grant DBI-0735191).

973

974 **Authors' contributions**

975 DHC, JNM and NRS conceived and designed the experiments. AR, DHC, RK,
976 LC, YI and KZ performed the experiments. AR, JMB and SDR analyzed the data.
977 AR, JMB, SDR, DHC and JNM contributed reagents/materials/analysis tools. AR,
978 JMB, SDR and NRS wrote the paper. All authors read and approved the final
979 manuscript.

980

981 **Figure legends:**

982 **Figure 1. Transcriptome profile of the tomato introgression lines.**

983 Differentially expressed genes at the transcript level for the ILs compared to
984 cultivated parent M82. Y-axis shows all the tomato genes starting from the first
985 gene on chromosome 1 to the last gene on chromosome 12, and X-axis depicts
986 the individual ILs. Genes differentially expressed within the introgression regions
987 (in *cis*) are shown as blue points and differentially expressed genes in *trans*
988 (outside) the introgression region are shown as orange points.

989

990 **Figure 2. *Cis*- and *Trans*-eQTL plotted by bin across the 12 chromosomes**

991 **of *S. lycopersicum* cv. M82.** A) Stacked bar graph showing the sum of the
992 number of eQTL mapping to each bin. B) Dotplot showing each eQTL arranged
993 vertically by bin and horizontally by the location of the transcript abundance
994 pattern it regulates. Bins with the largest numbers of *trans*-eQTL (4D, 4E, 4F, 6B,
995 6C, 8A, 8B) are highlighted by green boxes. C) Map of chromosomes 4, 6, and 8

996 showing the overlapping IL regions, which define the bins (Modified from
997 Chitwood et al., 2013). Bins with the largest numbers of *trans*-eQTL are indicated
998 by green asterisks.

999

1000 **Figure 3. BH-SNE 2D mapping of eQTL.** A) Forty-two distinct modules
1001 identified by DBscan from the mapping generated by BH-SNE analysis. B) The
1002 three modules defined as landmark modules: photosynthesis, defense and
1003 cysteine-type peptidase activity and the leaf development module's position
1004 within the mapping. Modules are false colored.

1005

1006 **Figure 4. Connections between eQTL and the genes with correlated**
1007 **transcript level.** Each plot includes the genes with eQTL that were clustered
1008 together into a module based on transcript level patterns. A) Defense module. B)
1009 Photosynthesis module. C) Cysteine peptidase module. D) Leaf development
1010 module. I) The 12 tomato chromosomes in megabases. II) Colored boxes
1011 indicate the sizes of each bin. III) Black bars indicate the locations of the genes.
1012 IV) Chords connect eQTL to the genes whose transcript level patterns they
1013 regulate. Chords are colored by the chromosome location of the eQTL.

1014

1015 **Figure 5. Median transcript level values for leaf development and**
1016 **photosynthesis related modules and expression correlation.** A) The median
1017 transcript level values of a module for each IL are shown. A consistent negative

1018 correlation between photosynthesis and Leaf development transcript expression
1019 is evident across nearly all 74 ILs. Dashed lines indicate one significant deviation
1020 from the module mean transcript level. Filled areas represent the median
1021 transcript level of the leaf development module, while open areas indicate the
1022 photosynthesis module median transcript levels. B) Leaf development median
1023 transcript level versus photosynthesis median transcript level values for each IL
1024 show a distinct negative correlation with an adjusted R-squared value of 0.77
1025 (calculated by linear regression in R).

1026

1027 **Figure 6. Enriched gene transcript levels that are controlled by specific**
1028 **bins.** A) Log fold change values (P1/SAM+P0) for previously identified
1029 differentially expressed genes with high transcript levels in the SAM + P0
1030 (magenta) vs. P1 (green). B) Scaled transcript level values for previously
1031 identified differentially expressed genes with increasing (red) and decreasing
1032 (blue) transcript levels over developmental time in the SAM + P0-P4. C) Scaled
1033 expression values for previously identified genes with differential levels of
1034 transcripts with increasing (orange) and decreasing (purple) transcript levels over
1035 developmental time in P5. D) Transcripts (y-axis) and bins (x-axis) showing the
1036 genetic regulation of transcript abundance (eQTL). Colors indicate SAM + P0
1037 (magenta) and P1 (green) transcripts. Bins enriched for genetically regulating
1038 genes with specific transcript expression patterns are indicated below with
1039 triangles. E) Same as in D), except showing genes with increasing (red) and

1040 decreasing (blue) transcript levels over temporal time in the SAM + P0-P4. F)
1041 Same as in D), except showing genes with increasing (orange) and decreasing
1042 (purple) transcript levels over temporal time in P5. Previously determined
1043 transcript abundance patterns are previously published (Chitwood et al., 2015).

1044

1045 **Figure 7. eQTL regulation of transcript abundance patterns that correlate**
1046 **with hypocotyl length.**

1047 A) Forty-two distinct modules identified by DBscan from the eQTL mapping
1048 generated by BH-SNE analysis. Modules enriched for genes with leaf
1049 development and photosynthesis GO terms are labeled in blue and green,
1050 respectively. Genes with transcript levels correlated with hypocotyl length under
1051 simulated shade are indicated by squares with positive correlations in red and
1052 negative correlations in yellow.

1053 B) Genes with transcript levels correlated with hypocotyl length under simulated
1054 shade are shown connected to their respective eQTL with chords. I) The 12
1055 tomato chromosomes in megabases. II) Colored boxes indicate the sizes of each
1056 bin. III) Black bars indicate the locations of the genes. IV) Chords connect eQTL
1057 to the genes whose transcript levels those eQTL regulate. Chords are colored by
1058 the chromosome location of the eQTL.

1059

1060

1061

References

- 1062
1063
1064 **Abe M, Katsumata H, Komeda Y, Takahashi T** (2003) Regulation of shoot
1065 epidermal cell differentiation by a pair of homeodomain proteins in
1066 Arabidopsis. *Development* **130**: 635-643
- 1067 **Abramoff MD, Magalhaes PJ, Ram SJ** (2004) Image Processing with ImageJ.
1068 *Biophotonics International* **11**: 36-42
- 1069 **Benjamini Y, Hochberg Y** (1995) Controlling the false discovery rate: A practical
1070 and powerful approach to multiple testing. *J R Stat Soc B* **57**: 289-300
- 1071 **Brem RB, Yvert G, Clinton R, Kruglyak L** (2002) Genetic dissection of
1072 transcriptional regulation in budding yeast. *Science* **296**: 752-755
- 1073 **Bushati N, Smith J, Briscoe J, Watkins C** (2011) An intuitive graphical
1074 visualization technique for the interrogation of transcriptome data. *Nucleic*
1075 *Acids Res* **39**: 7380-7389
- 1076 **Carles CC, Choffnes-Inada D, Reville K, Lertpiriyapong K, Fletcher JC**
1077 (2005) ULTRAPETALA1 encodes a SAND domain putative transcriptional
1078 regulator that controls shoot and floral meristem activity in Arabidopsis.
1079 *Development* **132**: 897-911
- 1080 **Chen X, Hackett CA, Niks RE, Hedley PE, Booth C, Druka A, Marcel TC, Vels**
1081 **A, Bayer M, Milne I, Morris J, Ramsay L, Marshall D, Cardle L, Waugh**
1082 **R** (2010) An eQTL analysis of partial resistance to Puccinia hordei in
1083 barley. *PLoS One* **5**: e8598
- 1084 **Chitwood DH, Kumar R, Headland LR, Ranjan A, Covington MF, Ichihashi Y,**
1085 **Fulop D, Jimenez-Gomez JM, Peng J, Maloof JN, Sinha NR** (2013) A
1086 quantitative genetic basis for leaf morphology in a set of precisely defined
1087 tomato introgression lines. *Plant Cell* **25**: 2465-2481
- 1088 **Chitwood DH, Kumar R, Ranjan A, Pelletier JM, Townsley BT, Ichihashi Y,**
1089 **Martinez CC, Zumstein K, Harada JJ, Maloof JN, Sinha NR** (2015)
1090 Light-Induced Indeterminacy Alters Shade-Avoiding Tomato Leaf
1091 Morphology. *Plant Physiol* **169**: 2030-2047
- 1092 **Chitwood DH, Ranjan A, Kumar R, Ichihashi Y, Zumstein K, Headland LR,**
1093 **Ostria-Gallardo E, Aguilar-Martinez JA, Bush S, Carriedo L, Fulop D,**
1094 **Martinez CC, Peng J, Maloof JN, Sinha NR** (2014) Resolving distinct
1095 genetic regulators of tomato leaf shape within a heteroblastic and
1096 ontogenetic context. *Plant Cell* **26**: 3616-3629
- 1097 **Chitwood DH, Sinha NR** (2013) A census of cells in time: quantitative genetics
1098 meets developmental biology. *Curr Opin Plant Biol* **16**: 92-99
- 1099 **Clark RM, Wagler TN, Quijada P, Doebley J** (2006) A distant upstream
1100 enhancer at the maize domestication gene *tb1* has pleiotropic effects on
1101 plant and inflorescent architecture. *Nat Genet* **38**: 594-597
- 1102 **Cnops G, Jover-Gil S, Peters JL, Neyt P, De Block S, Robles P, Ponce MR,**
1103 **Gerats T, Micol JL, Van Lijsebettens M** (2004) The *rotunda2* mutants
1104 identify a role for the *LEUNIG* gene in vegetative leaf morphogenesis. *J*
1105 *Exp Bot* **55**: 1529-1539

- 1106 **Cubillos FA, Coustham V, Loudet O** (2012) Lessons from eQTL mapping
1107 studies: non-coding regions and their role behind natural phenotypic
1108 variation in plants. *Curr Opin Plant Biol* **15**: 192-198
- 1109 **DeCook R, Lall S, Nettleton D, Howell SH** (2006) Genetic regulation of gene
1110 expression during shoot development in Arabidopsis. *Genetics* **172**: 1155-
1111 1164
- 1112 **Diaz-Mendoza M, Velasco-Arroyo B, Gonzalez-Melendi P, Martinez M, Diaz I**
1113 (2014) C1A cysteine protease-cystatin interactions in leaf senescence. *J*
1114 *Exp Bot* **65**: 3825-3833
- 1115 **Druka A, Potokina E, Luo Z, Jiang N, Chen X, Kearsley M, Waugh R** (2010)
1116 Expression quantitative trait loci analysis in plants. *Plant Biotechnol J* **8**:
1117 10-27
- 1118 **Eshed Y, Zamir D** (1995) An introgression line population of *Lycopersicon*
1119 *pennellii* in the cultivated tomato enables the identification and fine
1120 mapping of yield-associated QTL. *Genetics* **141**: 1147-1162
- 1121 **Frary A, Nesbitt TC, Grandillo S, Knaap E, Cong B, Liu J, Meller J, Elber R,**
1122 **Alpert KB, Tanksley SD** (2000) fw2.2: a quantitative trait locus key to the
1123 evolution of tomato fruit size. *Science* **289**: 85-88
- 1124 **Fridman E, Carrari F, Liu YS, Fernie AR, Zamir D** (2004) Zooming in on a
1125 quantitative trait for tomato yield using interspecific introgressions. *Science*
1126 **305**: 1786-1789
- 1127 **Fukao T, Xu K, Ronald PC, Bailey-Serres J** (2006) A variable cluster of
1128 ethylene response factor-like genes regulates metabolic and
1129 developmental acclimation responses to submergence in rice. *Plant Cell*
1130 **18**: 2021-2034
- 1131 **Fulop D, Ranjan A, Ofner I, Covington MF, Chitwood DH, West D, Ichihashi**
1132 **Y, Headland L, Zamir D, Maloof JN, Sinha NR** (2016) A new advanced
1133 backcross tomato population enables high resolution leaf QTL mapping
1134 and gene identification. bioRxiv 040923; doi:
1135 <http://dx.doi.org/10.1101/040923>
- 1136 **Goff SA, Vaughn M, McKay S, Lyons E, Stapleton AE, Gessler D, Matasci N,**
1137 **Wang L, Hanlon M, Lenards A, Muir A, Merchant N, Lowry S, Mock S,**
1138 **Helmke M, Kubach A, Narro M, Hopkins N, Micklos D, Hilgert U,**
1139 **Gonzales M, Jordan C, Skidmore E, Dooley R, Cazes J, McLay R, Lu**
1140 **Z, Pasternak S, Koesterke L, Piel WH, Grene R, Noutsos C, Gendler**
1141 **K, Feng X, Tang C, Lent M, Kim SJ, Kvilekval K, Manjunath BS,**
1142 **Tannen V, Stamatakis A, Sanderson M, Welch SM, Cranston KA,**
1143 **Soltis P, Soltis D, O'Meara B, Ane C, Brutnell T, Kleibenstein DJ,**
1144 **White JW, Leebens-Mack J, Donoghue MJ, Spalding EP, Vision TJ,**
1145 **Myers CR, Lowenthal D, Enquist BJ, Boyle B, Akoglu A, Andrews G,**
1146 **Ram S, Ware D, Stein L, Stanzione D** (2011) The iPlant Collaborative:
1147 Cyberinfrastructure for Plant Biology. *Front Plant Sci* **2**: 34
- 1148 **Hammond JP, Mayes S, Bowen HC, Graham NS, Hayden RM, Love CG,**
1149 **Spracklen WP, Wang J, Welham SJ, White PJ, King GJ, Broadley MR**

- 1150 (2011) Regulatory hotspots are associated with plant gene expression
1151 under varying soil phosphorus supply in *Brassica rapa*. *Plant Physiol* **156**:
1152 1230-1241
- 1153 **Hennig C** (2014) FPC: Flexible procedures for Clustering. R Package Version:
1154 2.1-9
- 1155 **Holloway B, Li B** (2010) Expression QTLs: applications for crop improvement.
1156 *Molecular Breeding* **26**: 381-391
- 1157 **Holtan HE, Hake S** (2003) Quantitative trait locus analysis of leaf dissection in
1158 tomato using *Lycopersicon pennellii* segmental introgression lines.
1159 *Genetics* **165**: 1541-1550
- 1160 **Ichihashi Y, Aguilar-Martinez JA, Farhi M, Chitwood DH, Kumar R, Millon**
1161 **LV, Peng J, Maloof JN, Sinha NR** (2014) Evolutionary developmental
1162 transcriptomics reveals a gene network module regulating interspecific
1163 diversity in plant leaf shape. *Proc Natl Acad Sci U S A* **111**: E2616-2621
- 1164 **Jansen RC, Nap JP** (2001) Genetical genomics: the added value from
1165 segregation. *Trends Genet* **17**: 388-391
- 1166 **Keurentjes JJ, Fu J, Terpstra IR, Garcia JM, van den Ackerveken G, Snoek**
1167 **LB, Peeters AJ, Vreugdenhil D, Koornneef M, Jansen RC** (2007)
1168 Regulatory network construction in *Arabidopsis* by using genome-wide
1169 gene expression quantitative trait loci. *Proc Natl Acad Sci U S A* **104**:
1170 1708-1713
- 1171 **Kliebenstein D** (2009) Quantitative genomics: analyzing intraspecific variation
1172 using global gene expression polymorphisms or eQTLs. *Annu Rev Plant*
1173 *Biol* **60**: 93-114
- 1174 **Kliebenstein DJ, West MA, van Leeuwen H, Kim K, Doerge RW, Michelmore**
1175 **RW, St Clair DA** (2006) Genomic survey of gene expression diversity in
1176 *Arabidopsis thaliana*. *Genetics* **172**: 1179-1189
- 1177 **Koenig D, Jimenez-Gomez JM, Kimura S, Fulop D, Chitwood DH, Headland**
1178 **LR, Kumar R, Covington MF, Devisetty UK, Tat AV, Tohge T, Bolger**
1179 **A, Schneeberger K, Ossowski S, Lanz C, Xiong G, Taylor-Teeple M,**
1180 **Brady SM, Pauly M, Weigel D, Usadel B, Fernie AR, Peng J, Sinha NR,**
1181 **Maloof JN** (2013) Comparative transcriptomics reveals patterns of
1182 selection in domesticated and wild tomato. *Proc Natl Acad Sci U S A* **110**:
1183 E2655-2662
- 1184 **Krijthe J** (2014) Rtsne: T-distributed Stochastic Neighbor Embedding using
1185 Barnes-Hut implementation. R Package Version: 0.9
- 1186 **Kroymann J, Donnerhacke S, Schnabelrauch D, Mitchell-Olds T** (2003)
1187 Evolutionary dynamics of an *Arabidopsis* insect resistance quantitative
1188 trait locus. *Proc Natl Acad Sci U S A* **100 Suppl 2**: 14587-14592
- 1189 **Kumar R, Ichihashi Y, Kimura S, Chitwood DH, Headland LR, Peng J,**
1190 **Maloof JN, Sinha NR** (2012) A High-Throughput Method for Illumina
1191 RNA-Seq Library Preparation. *Front Plant Sci* **3**: 202
- 1192 **Li H, Durbin R** (2009) Fast and accurate short read alignment with Burrows-
1193 Wheeler transform. *Bioinformatics* **25**: 1754-1760

- 1194 **Liu YS, Zamir D** (1999) Second generation *L. pennellii* introgression lines and
1195 the concept of bin mapping. *Tomato Genet. Coop. Rep.* **49**: 26-30
- 1196 **Longair MH, Baker DA, Armstrong JD** (2011) Simple Neurite Tracer: open
1197 source software for reconstruction, visualization and analysis of neuronal
1198 processes. *Bioinformatics* **27**: 2453-2454
- 1199 **Moyle LC** (2008) Ecological and evolutionary genomics in the wild tomatoes
1200 (*Solanum sect. Lycopersicon*). *Evolution* **62**: 2995-3013
- 1201 **Muir CD, Pease JB, Moyle LC** (2014) Quantitative genetic analysis indicates
1202 natural selection on leaf phenotypes across wild tomato species (*Solanum*
1203 *sect. Lycopersicon*; Solanaceae). *Genetics* **198**: 1629-1643
- 1204 **Muller NA, Wijnen CL, Srinivasan A, Ryngajlo M, Ofner I, Lin T, Ranjan A,**
1205 **West D, Maloof JN, Sinha NR, Huang S, Zamir D, Jimenez-Gomez JM**
1206 (2016) Domestication selected for deceleration of the circadian clock in
1207 cultivated tomato. *Nat Genet* **48**: 89-93
- 1208 **R Development CoreTeam** (2015) R: A Language and Environment for
1209 Statistical Computing. (Vienna, Austria: R Foundation for Statistical
1210 Computing)
- 1211 **Ranjan A, Ichihashi Y, Sinha NR** (2012) The tomato genome: implications for
1212 plant breeding, genomics and evolution. *Genome Biol* **13**: 167
- 1213 **Roberts A, Pachter L** (2013) Streaming fragment assignment for real-time
1214 analysis of sequencing experiments. *Nat Methods* **10**: 71-73
- 1215 **Robinson MD, Oshlack A** (2010) A scaling normalization method for differential
1216 expression analysis of RNA-seq data. *Genome Biol* **11**: R25
- 1217 **Schadt EE, Monks SA, Drake TA, Lusk AJ, Che N, Colinayo V, Ruff TG,**
1218 **Milligan SB, Lamb JR, Cavet G, Linsley PS, Mao M, Stoughton RB,**
1219 **Friend SH** (2003) Genetics of gene expression surveyed in maize, mouse
1220 and man. *Nature* **422**: 297-302
- 1221 **Sharlach M, Dahlbeck D, Liu L, Chiu J, Jimenez-Gomez JM, Kimura S,**
1222 **Koenig D, Maloof JN, Sinha N, Minsavage GV, Jones JB, Stall RE,**
1223 **Staskawicz BJ** (2013) Fine genetic mapping of RXopJ4, a bacterial spot
1224 disease resistance locus from *Solanum pennellii* LA716. *Theor Appl Genet*
1225 **126**: 601-609
- 1226 **Svistonoff S, Creff A, Reymond M, Sigoillot-Claude C, Ricaud L, Blanchet**
1227 **A, Nussaume L, Desnos T** (2007) Root tip contact with low-phosphate
1228 media reprograms plant root architecture. *Nat Genet* **39**: 792-796
- 1229 **van der Maaten L** (2013) Barnes-Hut-SNE. arXiv:1301.3342[cs.LG]
- 1230 **van der Maaten L, Hinton G** (2008) Visualizing Data using t-SNE. *Journal of*
1231 *Machine Learning Research* **9**: 2579-2605
- 1232 **Werner JD, Borevitz JO, Warthmann N, Trainer GT, Ecker JR, Chory J,**
1233 **Weigel D** (2005) Quantitative trait locus mapping and DNA array
1234 hybridization identify an FLM deletion as a cause for natural flowering-time
1235 variation. *Proc Natl Acad Sci U S A* **102**: 2460-2465
- 1236 **West MA, Kim K, Kliebenstein DJ, van Leeuwen H, Michelmore RW, Doerge**
1237 **RW, St Clair DA** (2007) Global eQTL mapping reveals the complex

- 1238 genetic architecture of transcript-level variation in Arabidopsis. *Genetics*
1239 **175**: 1441-1450
- 1240 **Wickham H** (2009) *ggplot2: elegant graphics for data analysis*. Springer New
1241 York
- 1242 **Young MD, Wakefield MJ, Smyth GK, Oshlack A** (2010) Gene ontology
1243 analysis for RNA-seq: accounting for selection bias. *Genome Biol* **11**: R14
- 1244 **Yu D, Chen C, Chen Z** (2001) Evidence for an important role of WRKY DNA
1245 binding proteins in the regulation of NPR1 gene expression. *Plant Cell* **13**:
1246 1527-1540
- 1247 **Zhang L, Fetch T, Nirmala J, Schmierer D, Brueggeman R, Steffenson B,**
1248 **Kleinhofs A** (2006) Rpr1, a gene required for Rpg1-dependent resistance
1249 to stem rust in barley. *Theor Appl Genet* **113**: 847-855

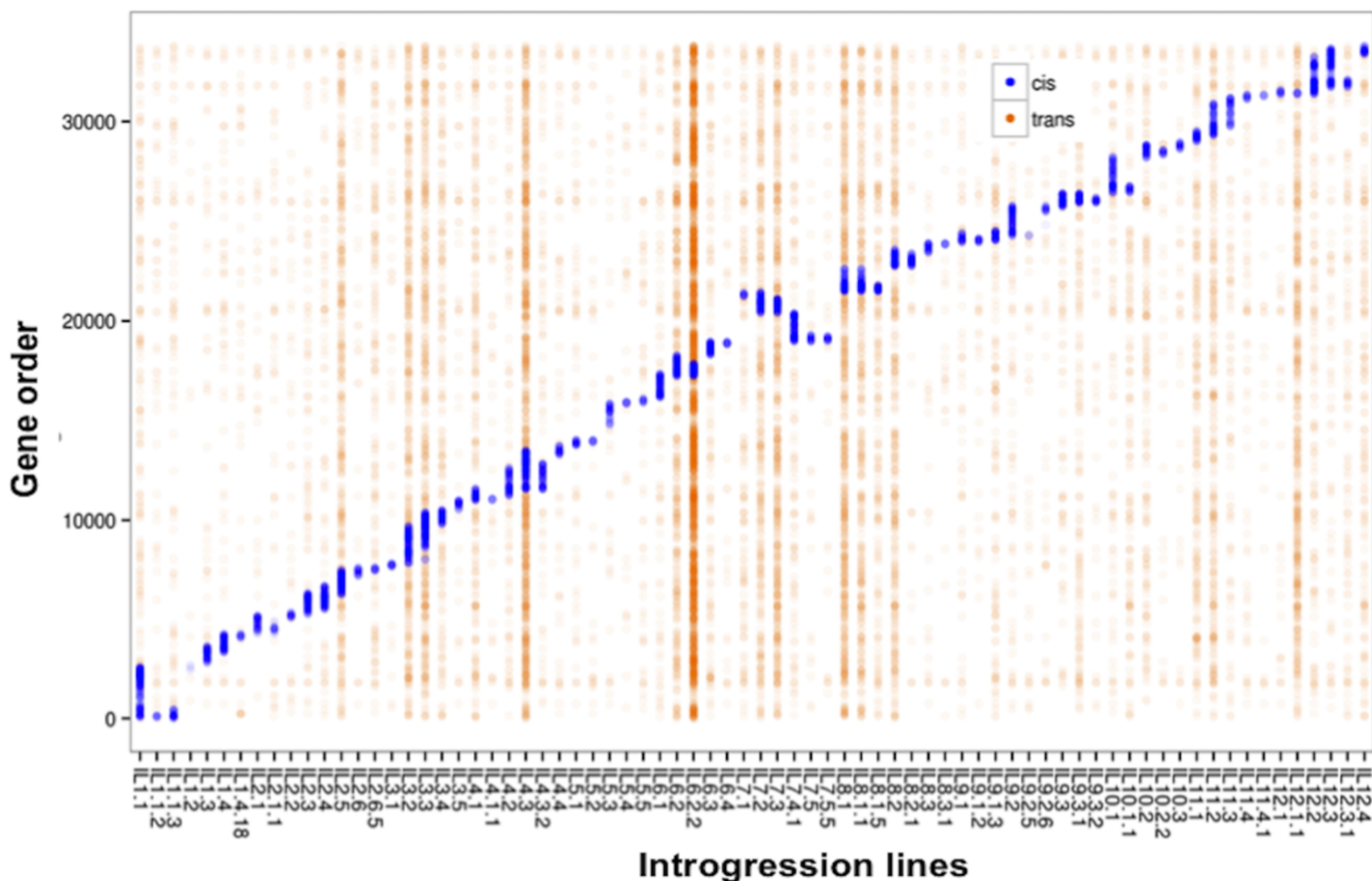


Figure 1. Transcriptome profile of the tomato introgression lines.

Differentially expressed genes at the transcript level for the ILs compared to cultivated parent M82. Y-axis shows all the tomato genes starting from the first gene on chromosome 1 to the last gene on chromosome 12, and X-axis depicts the individual ILs. Genes differentially expressed within the introgression regions (in *cis*) are shown as blue points and differentially expressed genes in *trans* (outside) the introgression region are shown as orange points.

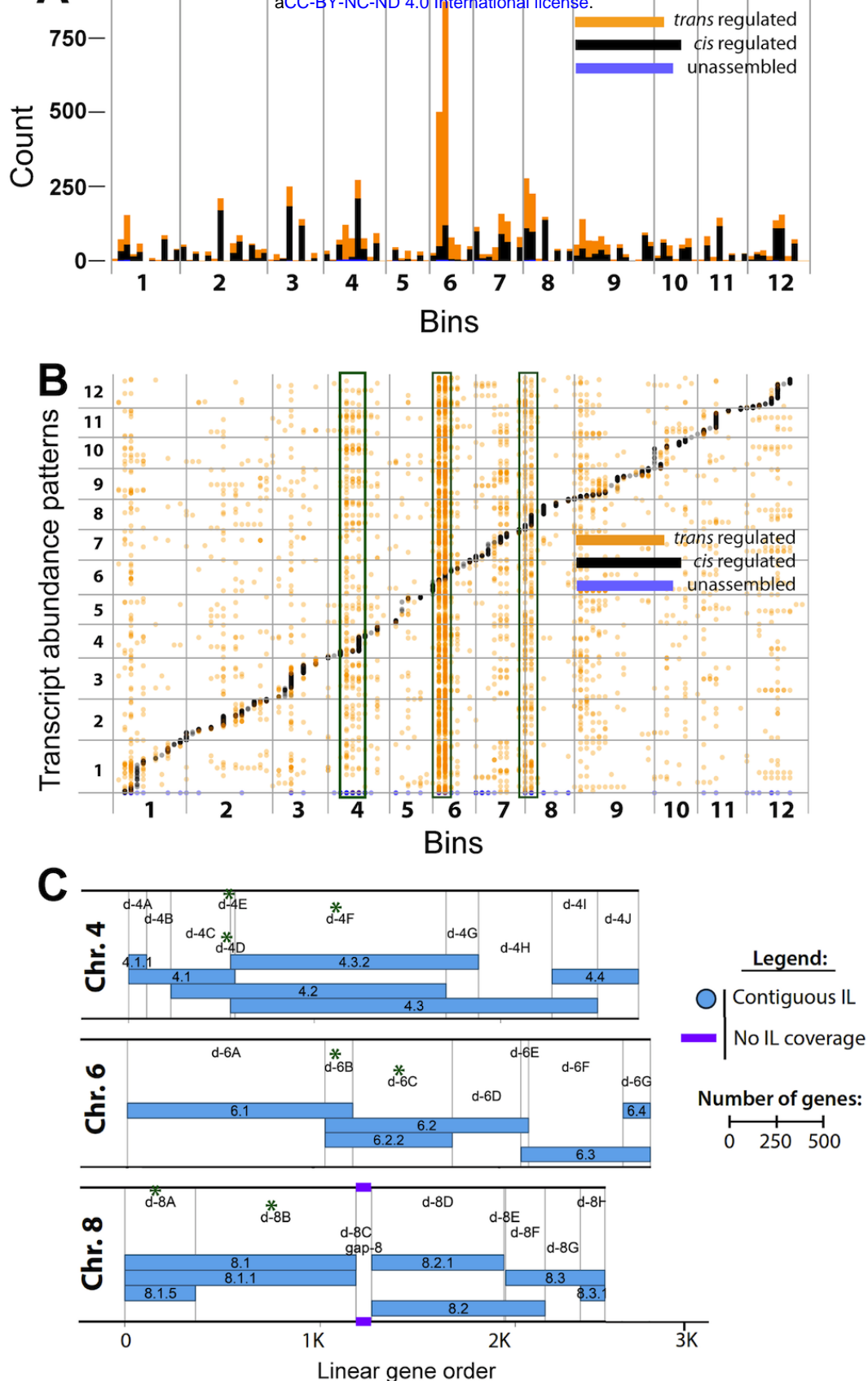


Figure 2. Cis- and Trans-eQTL plotted by bin across the 12 chromosomes of *S. lycopersicum* cv. M82. A) Stacked bar graph showing the sum of the number of eQTL mapping to each bin. B) Dotplot showing each eQTL arranged vertically by bin and horizontally by the location of the transcript abundance pattern it regulates. Bins with the largest numbers of *trans*-eQTL (4D, 4E, 4F, 6B, 6C, 8A, 8B) are highlighted by green boxes. C) Map of chromosomes 4, 6, and 8 showing the overlapping IL regions, which define the bins (Modified from Chitwood et al., 2013). Bins with the largest numbers of *trans*-eQTL are indicated by green asterisks.

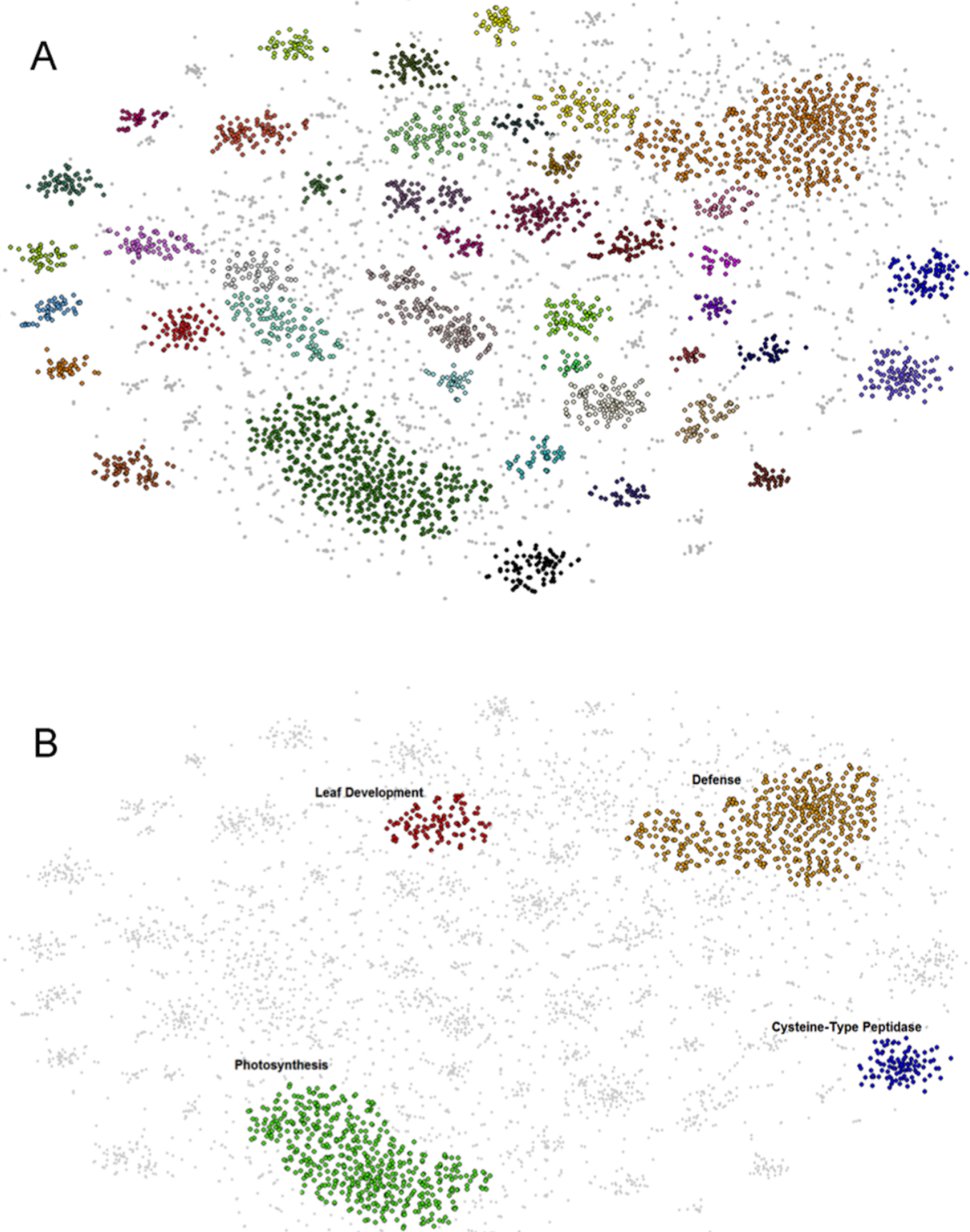


Figure 3. BH-SNE 2D mapping of eQTL. (A) Forty-two distinct modules identified by DBscan from the mapping generated by BH-SNE analysis. (B) The three modules defined as landmark modules: photosynthesis, defense and cysteine-type peptidase activity and the leaf development module's position within the mapping. Modules are false colored.

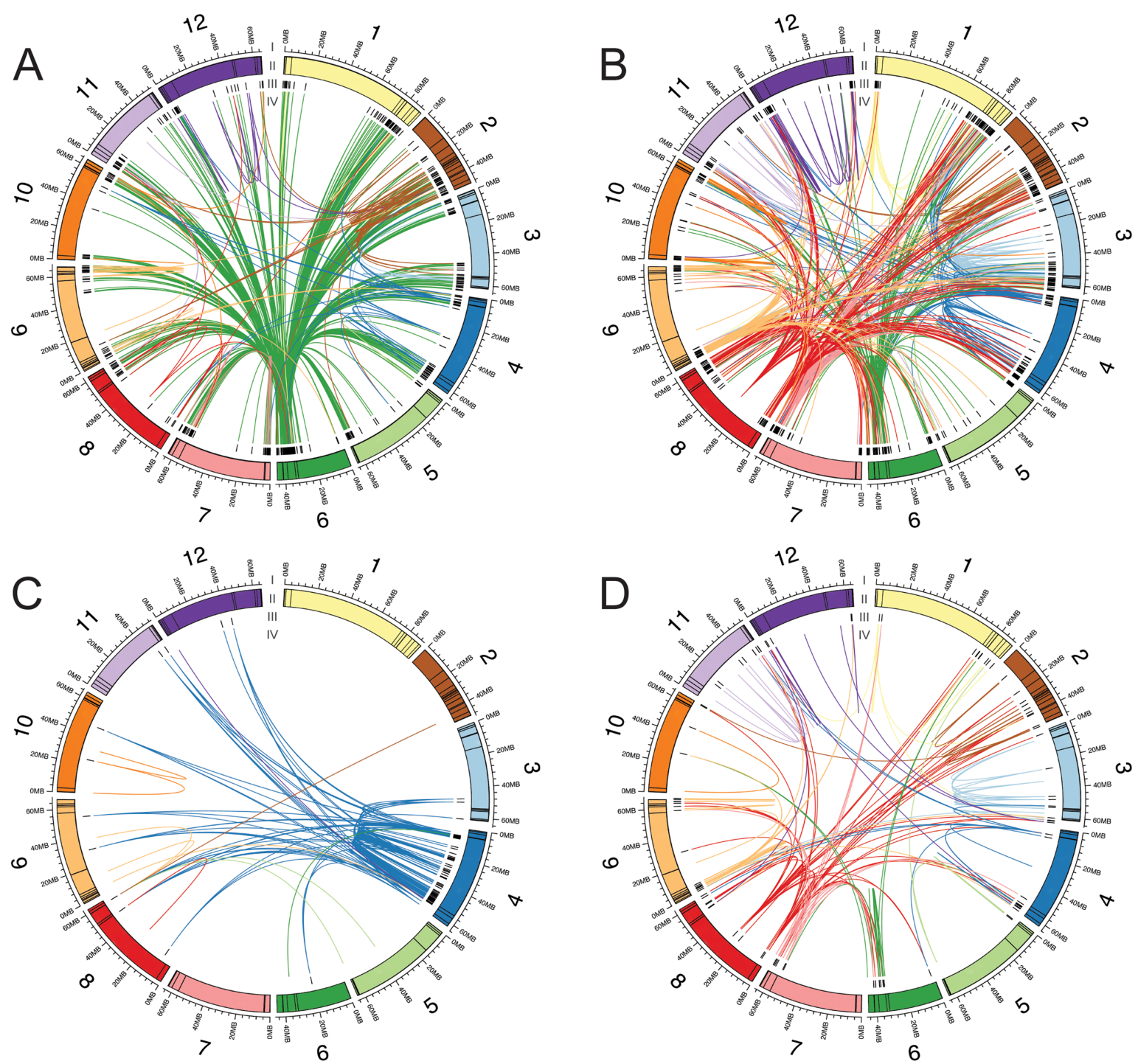


Figure 4. Connections between eQTL and the genes with correlated transcript level. Each plot includes the genes with eQTL that were clustered together into a module based on transcript level patterns. A) Defense module. B) Photosynthesis module. C) Cysteine peptidase module. D) Leaf development module. I) The 12 tomato chromosomes in megabases. II) Colored boxes indicate the sizes of each bin. III) Black bars indicate the locations of the genes. IV) Chords connect eQTL to the genes whose transcript level patterns they regulate. Chords are colored by the chromosome location of the eQTL.

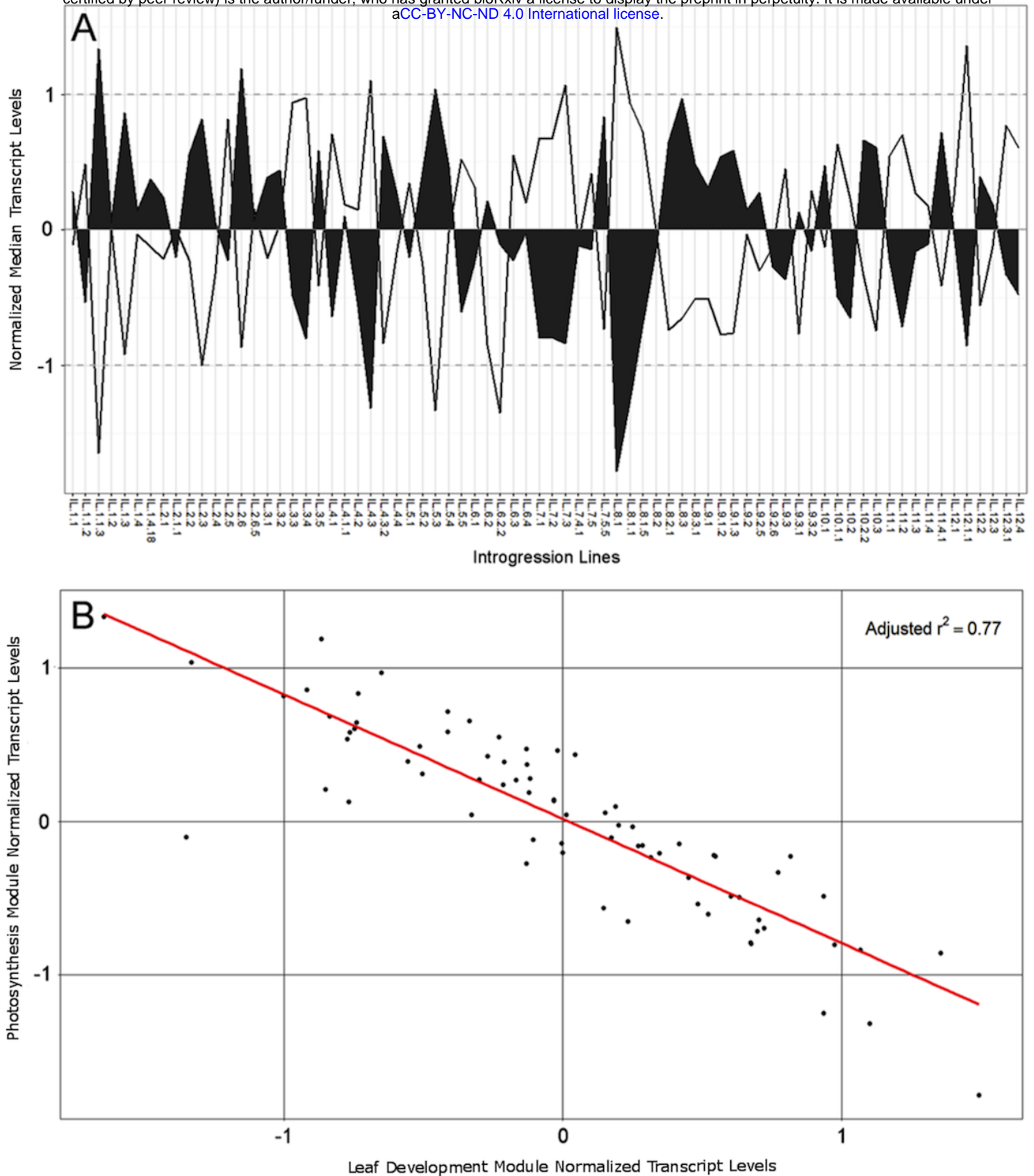


Figure 5. Median transcript level values for leaf development and photosynthesis related modules and transcript level correlation. A) The median transcript level values of a module for each IL are shown. A consistent negative correlation between photosynthesis and Leaf development transcript levels is evident across nearly all 74 ILs. Dashed lines indicate one significant deviation from the module mean transcript level. Filled areas represent the median transcript level of the leaf development module, while open areas indicate the photosynthesis module median transcript levels. B) Leaf development median transcript level versus photosynthesis median transcript level values for each IL show a distinct negative correlation with an adjusted R-squared value of 0.77 (calculated by linear regression in R).

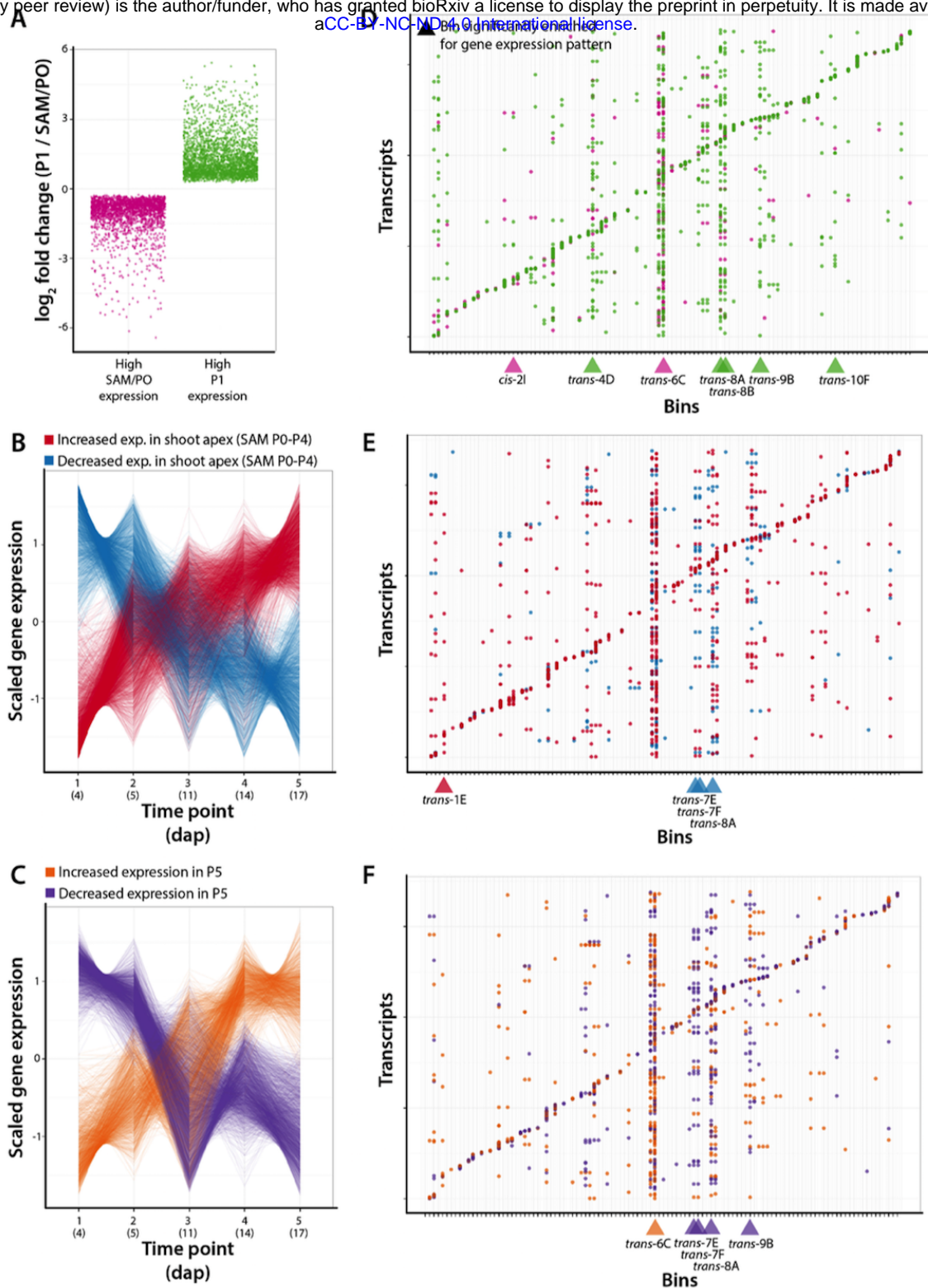


Figure 6. Enriched gene transcript levels that are controlled by specific bins.

A) Log fold change values (P1/SAM+P0) for previously identified differentially expressed genes with high transcript levels in the SAM + P0 (magenta) vs. P1 (green). B) Scaled transcript level values for previously identified differentially expressed genes with increasing (red) and decreasing (blue) transcript levels over developmental time in the SAM + P0-P4. C) Scaled expression values for previously identified genes with differential levels of transcripts with increasing (orange) and decreasing (purple) transcript levels over developmental time in P5. D) Transcripts (y-axis) and bins (x-axis) showing the genetic regulation of transcript abundance (eQTL). Colors indicate SAM + P0 (magenta) and P1 (green) transcripts. Bins enriched for genetically regulating genes with specific transcript expression patterns are indicated below with triangles. E) Same as in D), except showing genes with increasing (red) and decreasing (blue) transcript levels over temporal time in the SAM + P0-P4. F) Same as in D), except showing genes with increasing (orange) and decreasing (purple) transcript levels over temporal time in P5. Previously determined transcript abundance patterns are previously published (Chitwood et al., 2015).

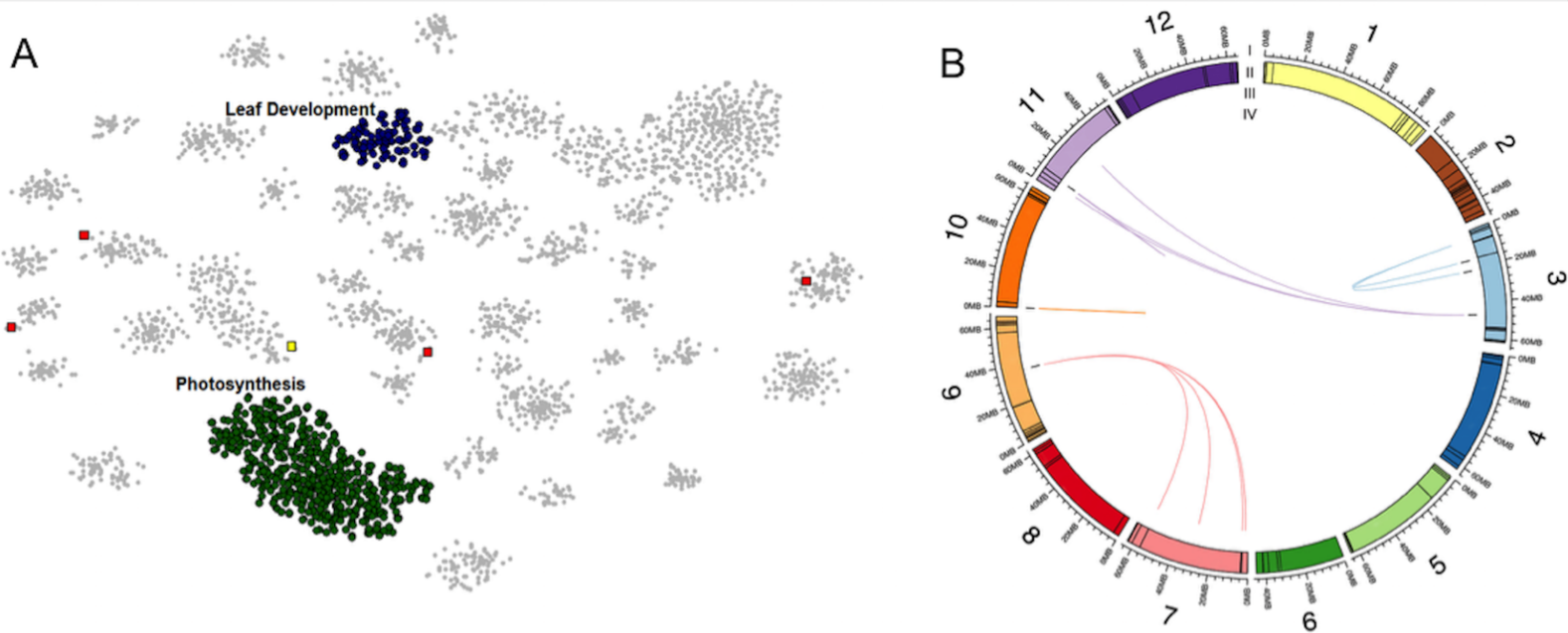


Figure 7. eQTL regulation of transcript abundance patterns that correlate with hypocotyl length.

A) Forty-two distinct modules identified by DBscan from the eQTL mapping generated by BH-SNE analysis. Modules enriched for genes with leaf development and photosynthesis GO terms are labeled in blue and green, respectively. Genes with transcript levels correlated with hypocotyl length under simulated shade are indicated by squares with positive correlations in red and negative correlations in yellow.

B) Genes with transcript levels correlated with hypocotyl length under simulated shade are shown connected to their respective eQTL with chords. I) The 12 tomato chromosomes in megabases. II) Colored boxes indicate the sizes of each bin. III) Black bars indicate the locations of the genes. IV) Chords connect eQTL to the genes whose transcript levels those eQTL regulate. Chords are colored by the chromosome location of the eQTL.

Parsed Citations

bioRxiv preprint doi: <https://doi.org/10.1101/040592>; this version posted July 8, 2016. The copyright holder for this preprint (which was not certified by peer review) is the author/funder, who has granted bioRxiv a license to display the preprint in perpetuity. It is made available under aCC-BY-NC-ND 4.0 International license.

Abe M, Katsumata H, Komeda Y, Takahashi T (2003) Regulation of shoot epidermal cell differentiation by a pair of homeodomain proteins in Arabidopsis. Development 130: 635-643

Pubmed: [Author and Title](#)

CrossRef: [Author and Title](#)

Google Scholar: [Author Only](#) [Title Only](#) [Author and Title](#)

Abramoff MD, Magalhaes PJ, Ram SJ (2004) Image Processing with ImageJ. Biophotonics International 11: 36-42

Pubmed: [Author and Title](#)

CrossRef: [Author and Title](#)

Google Scholar: [Author Only](#) [Title Only](#) [Author and Title](#)

Benjamini Y, Hochberg Y (1995) Controlling the false discovery rate: A practical and powerful approach to multiple testing. J R Stat Soc B 57: 289-300

Pubmed: [Author and Title](#)

CrossRef: [Author and Title](#)

Google Scholar: [Author Only](#) [Title Only](#) [Author and Title](#)

Brem RB, Yvert G, Clinton R, Kruglyak L (2002) Genetic dissection of transcriptional regulation in budding yeast. Science 296: 752-755

Pubmed: [Author and Title](#)

CrossRef: [Author and Title](#)

Google Scholar: [Author Only](#) [Title Only](#) [Author and Title](#)

Bushati N, Smith J, Briscoe J, Watkins C (2011) An intuitive graphical visualization technique for the interrogation of transcriptome data. Nucleic Acids Res 39: 7380-7389

Pubmed: [Author and Title](#)

CrossRef: [Author and Title](#)

Google Scholar: [Author Only](#) [Title Only](#) [Author and Title](#)

Carles CC, Choffnes-Inada D, Reville K, Lertpiriyapong K, Fletcher JC (2005) ULTRAPETALA1 encodes a SAND domain putative transcriptional regulator that controls shoot and floral meristem activity in Arabidopsis. Development 132: 897-911

Pubmed: [Author and Title](#)

CrossRef: [Author and Title](#)

Google Scholar: [Author Only](#) [Title Only](#) [Author and Title](#)

Chen X, Hackett CA, Niks RE, Hedley PE, Booth C, Druka A, Marcel TC, Vels A, Bayer M, Milne I, Morris J, Ramsay L, Marshall D, Cardle L, Waugh R (2010) An eQTL analysis of partial resistance to Puccinia hordei in barley. PLoS One 5: e8598

Pubmed: [Author and Title](#)

CrossRef: [Author and Title](#)

Google Scholar: [Author Only](#) [Title Only](#) [Author and Title](#)

Chitwood DH, Kumar R, Headland LR, Ranjan A, Covington MF, Ichihashi Y, Fulop D, Jimenez-Gomez JM, Peng J, Maloof JN, Sinha NR (2013) A quantitative genetic basis for leaf morphology in a set of precisely defined tomato introgression lines. Plant Cell 25: 2465-2481

Pubmed: [Author and Title](#)

CrossRef: [Author and Title](#)

Google Scholar: [Author Only](#) [Title Only](#) [Author and Title](#)

Chitwood DH, Kumar R, Ranjan A, Pelletier JM, Townsley BT, Ichihashi Y, Martinez CC, Zumstein K, Harada JJ, Maloof JN, Sinha NR (2015) Light-Induced Indeterminacy Alters Shade-Avoiding Tomato Leaf Morphology. Plant Physiol 169: 2030-2047

Pubmed: [Author and Title](#)

CrossRef: [Author and Title](#)

Google Scholar: [Author Only](#) [Title Only](#) [Author and Title](#)

Chitwood DH, Ranjan A, Kumar R, Ichihashi Y, Zumstein K, Headland LR, Ostria-Gallardo E, Aguilar-Martinez JA, Bush S, Carriedo L, Fulop D, Martinez CC, Peng J, Maloof JN, Sinha NR (2014) Resolving distinct genetic regulators of tomato leaf shape within a heteroblastic and ontogenetic context. Plant Cell 26: 3616-3629

Pubmed: [Author and Title](#)

CrossRef: [Author and Title](#)

Google Scholar: [Author Only](#) [Title Only](#) [Author and Title](#)

Chitwood DH, Sinha NR (2013) A census of cells in time: quantitative genetics meets developmental biology. Curr Opin Plant Biol 16: 92-99

Pubmed: [Author and Title](#)

CrossRef: [Author and Title](#)

Google Scholar: [Author Only](#) [Title Only](#) [Author and Title](#)

Clark RM, Wagler TN, Quijada P, Doebley J (2006) A distant upstream enhancer at the maize domestication gene tb1 has pleiotropic effects on plant and inflorescent architecture. Nat Genet 38: 594-597

Pubmed: [Author and Title](#)

CrossRef: [Author and Title](#)

Google Scholar: [Author Only](#) [Title Only](#) [Author and Title](#)

Cnops G, Jover-Gil S, Peters JL, Neyt P, De Block S, Robles P, Ponce MR, Gerats T, Micol JL, Van Lijsebettens M (2004) The rotunda2 mutants identify a role for the LEUNIG gene in vegetative leaf morphogenesis. J Exp Bot 55: 1529-1539

Pubmed: [Author and Title](#)

CrossRef: [Author and Title](#)

Google Scholar: [Author Only](#) [Title Only](#) [Author and Title](#)

Cubillos FA, Coustham V, Loudet O (2012) Lessons from eQTL mapping studies: non-coding regions and their role behind natural phenotypic variation in plants. *Curr Opin Plant Biol* 15: 192-198
bioRxiv preprint doi: <https://doi.org/10.1101/049592>; this version posted July 8, 2016. The copyright holder for this preprint (which was not certified by peer review) is the author/funder, who has granted bioRxiv a license to display the preprint in perpetuity. It is made available under aCC-BY-NC-ND 4.0 International license.

Pubmed: [Author and Title](#)

CrossRef: [Author and Title](#)

Google Scholar: [Author Only](#) [Title Only](#) [Author and Title](#)

DeCook R, Lall S, Nettleton D, Howell SH (2006) Genetic regulation of gene expression during shoot development in Arabidopsis. *Genetics* 172: 1155-1164

Pubmed: [Author and Title](#)

CrossRef: [Author and Title](#)

Google Scholar: [Author Only](#) [Title Only](#) [Author and Title](#)

Diaz-Mendoza M, Velasco-Arroyo B, Gonzalez-Melendi P, Martinez M, Diaz I (2014) C1A cysteine protease-cystatin interactions in leaf senescence. *J Exp Bot* 65: 3825-3833

Pubmed: [Author and Title](#)

CrossRef: [Author and Title](#)

Google Scholar: [Author Only](#) [Title Only](#) [Author and Title](#)

Druka A, Potokina E, Luo Z, Jiang N, Chen X, Kearsley M, Waugh R (2010) Expression quantitative trait loci analysis in plants. *Plant Biotechnol J* 8: 10-27

Pubmed: [Author and Title](#)

CrossRef: [Author and Title](#)

Google Scholar: [Author Only](#) [Title Only](#) [Author and Title](#)

Eshed Y, Zamir D (1995) An introgression line population of *Lycopersicon pennellii* in the cultivated tomato enables the identification and fine mapping of yield-associated QTL. *Genetics* 141: 1147-1162

Pubmed: [Author and Title](#)

CrossRef: [Author and Title](#)

Google Scholar: [Author Only](#) [Title Only](#) [Author and Title](#)

Frary A, Nesbitt TC, Grandillo S, Knaap E, Cong B, Liu J, Meller J, Elber R, Alpert KB, Tanksley SD (2000) fw2.2: a quantitative trait locus key to the evolution of tomato fruit size. *Science* 289: 85-88

Pubmed: [Author and Title](#)

CrossRef: [Author and Title](#)

Google Scholar: [Author Only](#) [Title Only](#) [Author and Title](#)

Fridman E, Carrari F, Liu YS, Fernie AR, Zamir D (2004) Zooming in on a quantitative trait for tomato yield using interspecific introgressions. *Science* 305: 1786-1789

Pubmed: [Author and Title](#)

CrossRef: [Author and Title](#)

Google Scholar: [Author Only](#) [Title Only](#) [Author and Title](#)

Fukao T, Xu K, Ronald PC, Bailey-Serres J (2006) A variable cluster of ethylene response factor-like genes regulates metabolic and developmental acclimation responses to submergence in rice. *Plant Cell* 18: 2021-2034

Pubmed: [Author and Title](#)

CrossRef: [Author and Title](#)

Google Scholar: [Author Only](#) [Title Only](#) [Author and Title](#)

Fulop D, Ranjan A, Ofner I, Covington MF, Chitwood DH, West D, Ichihashi Y, Headland L, Zamir D, Maloof JN, Sinha NR (2016) A new advanced backcross tomato population enables high resolution leaf QTL mapping and gene identification. *bioRxiv* 040923; doi: <http://dx.doi.org/10.1101/040923>

Pubmed: [Author and Title](#)

CrossRef: [Author and Title](#)

Google Scholar: [Author Only](#) [Title Only](#) [Author and Title](#)

Goff SA, Vaughn M, McKay S, Lyons E, Stapleton AE, Gessler D, Matasci N, Wang L, Hanlon M, Lenards A, Muir A, Merchant N, Lowry S, Mock S, Helmke M, Kubach A, Narro M, Hopkins N, Micklos D, Hilgert U, Gonzales M, Jordan C, Skidmore E, Dooley R, Cazes J, McLay R, Lu Z, Pasternak S, Koesterke L, Piel WH, Grene R, Noutsos C, Gendler K, Feng X, Tang C, Lent M, Kim SJ, Kvilekval K, Manjunath BS, Tannen V, Stamatakis A, Sanderson M, Welch SM, Cranston KA, Soltis P, Soltis D, O'Meara B, Ane C, Brutnell T, Kleibenstein DJ, White JW, Leebens-Mack J, Donoghue MJ, Spalding EP, Vision TJ, Myers CR, Lowenthal D, Enquist BJ, Boyle B, Akoglu A, Andrews G, Ram S, Ware D, Stein L, Stanzione D (2011) The iPlant Collaborative: Cyberinfrastructure for Plant Biology. *Front Plant Sci* 2: 34

Pubmed: [Author and Title](#)

CrossRef: [Author and Title](#)

Google Scholar: [Author Only](#) [Title Only](#) [Author and Title](#)

Hammond JP, Mayes S, Bowen HC, Graham NS, Hayden RM, Love CG, Spracklen WP, Wang J, Welham SJ, White PJ, King GJ, Broadley MR (2011) Regulatory hotspots are associated with plant gene expression under varying soil phosphorus supply in *Brassica rapa*. *Plant Physiol* 156: 1230-1241

Pubmed: [Author and Title](#)

CrossRef: [Author and Title](#)

Google Scholar: [Author Only](#) [Title Only](#) [Author and Title](#)

Hennig C (2014) FPC: Flexible procedures for Clustering. R Package Version: 2.1-9

Pubmed: [Author and Title](#)

CrossRef: [Author and Title](#)

Google Scholar: [Author Only](#) [Title Only](#) [Author and Title](#)

Holloway B, Li B (2010) Expression QTLs: applications for crop improvement. Molecular Breeding 26: 381-391

Pubmed: [Author and Title](#)

CrossRef: [Author and Title](#)

Google Scholar: [Author Only Title Only Author and Title](#)
bioRxiv preprint doi: <https://doi.org/10.1101/040592>; this version posted July 8, 2016. The copyright holder for this preprint (which was not certified by peer review) is the author/funder, who has granted bioRxiv a license to display the preprint in perpetuity. It is made available under aCC-BY-NC-ND 4.0 International license.

Holtan HE, Hake S (2003) Quantitative trait locus analysis of leaf dissection in tomato using Lycopersicon pennellii segmental introgression lines. Genetics 165: 1541-1550

Pubmed: [Author and Title](#)

CrossRef: [Author and Title](#)

Google Scholar: [Author Only Title Only Author and Title](#)

Ichihashi Y, Aguilar-Martinez JA, Farhi M, Chitwood DH, Kumar R, Millon LV, Peng J, Maloof JN, Sinha NR (2014) Evolutionary developmental transcriptomics reveals a gene network module regulating interspecific diversity in plant leaf shape. Proc Natl Acad Sci U S A 111: E2616-2621

Pubmed: [Author and Title](#)

CrossRef: [Author and Title](#)

Google Scholar: [Author Only Title Only Author and Title](#)

Jansen RC, Nap JP (2001) Genetical genomics: the added value from segregation. Trends Genet 17: 388-391

Pubmed: [Author and Title](#)

CrossRef: [Author and Title](#)

Google Scholar: [Author Only Title Only Author and Title](#)

Keurentjes JJ, Fu J, Terpstra IR, Garcia JM, van den Ackerveken G, Snoek LB, Peeters AJ, Vreugdenhil D, Koornneef M, Jansen RC (2007) Regulatory network construction in Arabidopsis by using genome-wide gene expression quantitative trait loci. Proc Natl Acad Sci U S A 104: 1708-1713

Pubmed: [Author and Title](#)

CrossRef: [Author and Title](#)

Google Scholar: [Author Only Title Only Author and Title](#)

Kliebenstein D (2009) Quantitative genomics: analyzing intraspecific variation using global gene expression polymorphisms or eQTLs. Annu Rev Plant Biol 60: 93-114

Pubmed: [Author and Title](#)

CrossRef: [Author and Title](#)

Google Scholar: [Author Only Title Only Author and Title](#)

Kliebenstein DJ, West MA, van Leeuwen H, Kim K, Doerge RW, Michelmore RW, St Clair DA (2006) Genomic survey of gene expression diversity in Arabidopsis thaliana. Genetics 172: 1179-1189

Pubmed: [Author and Title](#)

CrossRef: [Author and Title](#)

Google Scholar: [Author Only Title Only Author and Title](#)

Koenig D, Jimenez-Gomez JM, Kimura S, Fulop D, Chitwood DH, Headland LR, Kumar R, Covington MF, Devisetty UK, Tat AV, Tohge T, Bolger A, Schneeberger K, Ossowski S, Lanz C, Xiong G, Taylor-Teeple M, Brady SM, Pauly M, Weigel D, Usadel B, Fernie AR, Peng J, Sinha NR, Maloof JN (2013) Comparative transcriptomics reveals patterns of selection in domesticated and wild tomato. Proc Natl Acad Sci U S A 110: E2655-2662

Pubmed: [Author and Title](#)

CrossRef: [Author and Title](#)

Google Scholar: [Author Only Title Only Author and Title](#)

Krijthe J (2014) Rtsne: T-distributed Stochastic Neighbor Embedding using Barnes-Hut implementation. R Package Version: 0.9

Pubmed: [Author and Title](#)

CrossRef: [Author and Title](#)

Google Scholar: [Author Only Title Only Author and Title](#)

Kroymann J, Donnerhacke S, Schnabelrauch D, Mitchell-Olds T (2003) Evolutionary dynamics of an Arabidopsis insect resistance quantitative trait locus. Proc Natl Acad Sci U S A 100 Suppl 2: 14587-14592

Pubmed: [Author and Title](#)

CrossRef: [Author and Title](#)

Google Scholar: [Author Only Title Only Author and Title](#)

Kumar R, Ichihashi Y, Kimura S, Chitwood DH, Headland LR, Peng J, Maloof JN, Sinha NR (2012) A High-Throughput Method for Illumina RNA-Seq Library Preparation. Front Plant Sci 3: 202

Pubmed: [Author and Title](#)

CrossRef: [Author and Title](#)

Google Scholar: [Author Only Title Only Author and Title](#)

Li H, Durbin R (2009) Fast and accurate short read alignment with Burrows-Wheeler transform. Bioinformatics 25: 1754-1760

Pubmed: [Author and Title](#)

CrossRef: [Author and Title](#)

Google Scholar: [Author Only Title Only Author and Title](#)

Liu YS, Zamir D (1999) Second generation L. pennellii introgression lines and the concept of bin mapping. Tomato Genet. Coop. Rep. 49: 26-30

Pubmed: [Author and Title](#)

CrossRef: [Author and Title](#)

Google Scholar: [Author Only Title Only Author and Title](#)

Longair MH, Baker DA, Armstrong JD (2011) Simple Neurite Tracer: open source software for reconstruction, visualization and analysis of neuronal processes. Bioinformatics 27: 2453-2454

Pubmed: [Author and Title](#)

CrossRef: [Author and Title](#)

Google Scholar: [Author Only Title Only Author and Title](#)

bioRxiv preprint doi: <https://doi.org/10.1101/040592>; this version posted July 8, 2016. The copyright holder for this preprint (which was not certified by peer review) is the author/funder, who has granted bioRxiv a license to display the preprint in perpetuity. It is made available under aCC-BY-NC-ND 4.0 International license.

Moyle LC (2008) Ecological and evolutionary genomics of the wild tomatoes (Solanum sect. Lycopersicon). Evolution 62: 295-303

Pubmed: [Author and Title](#)

CrossRef: [Author and Title](#)

Google Scholar: [Author Only Title Only Author and Title](#)

Muir CD, Pease JB, Moyle LC (2014) Quantitative genetic analysis indicates natural selection on leaf phenotypes across wild tomato species (Solanum sect. Lycopersicon; Solanaceae). Genetics 198: 1629-1643

Pubmed: [Author and Title](#)

CrossRef: [Author and Title](#)

Google Scholar: [Author Only Title Only Author and Title](#)

Muller NA, Wijnen CL, Srinivasan A, Ryngajlo M, Ofner I, Lin T, Ranjan A, West D, Maloof JN, Sinha NR, Huang S, Zamir D, Jimenez-Gomez JM (2016) Domestication selected for deceleration of the circadian clock in cultivated tomato. Nat Genet 48: 89-93

Pubmed: [Author and Title](#)

CrossRef: [Author and Title](#)

Google Scholar: [Author Only Title Only Author and Title](#)

R Development CoreTeam (2015) R: A Language and Environment for Statistical Computing. (Vienna, Austria: R Foundation for Statistical Computing)

Pubmed: [Author and Title](#)

CrossRef: [Author and Title](#)

Google Scholar: [Author Only Title Only Author and Title](#)

Ranjan A, Ichihashi Y, Sinha NR (2012) The tomato genome: implications for plant breeding, genomics and evolution. Genome Biol 13: 167

Pubmed: [Author and Title](#)

CrossRef: [Author and Title](#)

Google Scholar: [Author Only Title Only Author and Title](#)

Roberts A, Pachter L (2013) Streaming fragment assignment for real-time analysis of sequencing experiments. Nat Methods 10: 71-73

Pubmed: [Author and Title](#)

CrossRef: [Author and Title](#)

Google Scholar: [Author Only Title Only Author and Title](#)

Robinson MD, Oshlack A (2010) A scaling normalization method for differential expression analysis of RNA-seq data. Genome Biol 11: R25

Pubmed: [Author and Title](#)

CrossRef: [Author and Title](#)

Google Scholar: [Author Only Title Only Author and Title](#)

Schadt EE, Monks SA, Drake TA, Lusk AJ, Che N, Colinayo V, Ruff TG, Milligan SB, Lamb JR, Cavet G, Linsley PS, Mao M, Stoughton RB, Friend SH (2003) Genetics of gene expression surveyed in maize, mouse and man. Nature 422: 297-302

Pubmed: [Author and Title](#)

CrossRef: [Author and Title](#)

Google Scholar: [Author Only Title Only Author and Title](#)

Sharlach M, Dahlbeck D, Liu L, Chiu J, Jimenez-Gomez JM, Kimura S, Koenig D, Maloof JN, Sinha N, Minsavage GV, Jones JB, Stall RE, Staskawicz BJ (2013) Fine genetic mapping of RXopJ4, a bacterial spot disease resistance locus from Solanum pennellii LA716. Theor Appl Genet 126: 601-609

Pubmed: [Author and Title](#)

CrossRef: [Author and Title](#)

Google Scholar: [Author Only Title Only Author and Title](#)

Svistonoff S, Creff A, Reymond M, Sigoillot-Claude C, Ricaud L, Blanchet A, Nussaume L, Desnos T (2007) Root tip contact with low-phosphate media reprograms plant root architecture. Nat Genet 39: 792-796

Pubmed: [Author and Title](#)

CrossRef: [Author and Title](#)

Google Scholar: [Author Only Title Only Author and Title](#)

van der Maaten L (2013) Barnes-Hut-SNE. arXiv:1301.3342[cs.LG]

Pubmed: [Author and Title](#)

CrossRef: [Author and Title](#)

Google Scholar: [Author Only Title Only Author and Title](#)

van der Maaten L, Hinton G (2008) Visualizing Data using t-SNE. Journal of Machine Learning Research 9: 2579-2605

Pubmed: [Author and Title](#)

CrossRef: [Author and Title](#)

Google Scholar: [Author Only Title Only Author and Title](#)

Werner JD, Borevitz JO, Warthmann N, Trainer GT, Ecker JR, Chory J, Weigel D (2005) Quantitative trait locus mapping and DNA array hybridization identify an FLM deletion as a cause for natural flowering-time variation. Proc Natl Acad Sci U S A 102: 2460-2465

Pubmed: [Author and Title](#)

CrossRef: [Author and Title](#)

Google Scholar: [Author Only Title Only Author and Title](#)

West MA, Kim K, Kliebenstein DJ, van Leeuwen H, Michelmore RW, Doerge RW, St Clair DA (2007) Global eQTL mapping reveals

the complex genetic architecture of transcript-level variation in Arabidopsis. Genetics 175: 1441-1450

Pubmed: [Author and Title](#)

CrossRef: [Author and Title](#)

Google Scholar: [Author Only](#) [Title Only](#) [Author and Title](#)
bioRxiv preprint doi: <https://doi.org/10.1101/040592>; this version posted July 8, 2016. The copyright holder for this preprint (which was not certified by peer review) is the author/funder, who has granted bioRxiv a license to display the preprint in perpetuity. It is made available under aCC-BY-NC-ND 4.0 International license.

Wickham H (2009) ggplot2: elegant graphics for data analysis. Springer New York

Pubmed: [Author and Title](#)

CrossRef: [Author and Title](#)

Google Scholar: [Author Only](#) [Title Only](#) [Author and Title](#)

Young MD, Wakefield MJ, Smyth GK, Oshlack A (2010) Gene ontology analysis for RNA-seq: accounting for selection bias. Genome Biol 11: R14

Pubmed: [Author and Title](#)

CrossRef: [Author and Title](#)

Google Scholar: [Author Only](#) [Title Only](#) [Author and Title](#)

Yu D, Chen C, Chen Z (2001) Evidence for an important role of WRKY DNA binding proteins in the regulation of NPR1 gene expression. Plant Cell 13: 1527-1540

Pubmed: [Author and Title](#)

CrossRef: [Author and Title](#)

Google Scholar: [Author Only](#) [Title Only](#) [Author and Title](#)

Zhang L, Fetch T, Nirmala J, Schmierer D, Brueggeman R, Steffenson B, Kleinhofs A (2006) Rpr1, a gene required for Rpg1-dependent resistance to stem rust in barley. Theor Appl Genet 113: 847-855

Pubmed: [Author and Title](#)

CrossRef: [Author and Title](#)

Google Scholar: [Author Only](#) [Title Only](#) [Author and Title](#)